Meteorological analysis and historical perspective of the 1999–2005 Canadian Prairie drought

by

Lisa Hryciw

Department of Atmospheric and Oceanic Sciences

McGill University, Montréal

July 2010

A thesis submitted to McGill University in partial fulfillment of the requirements of the degree of Master of Science

©Lisa Hryciw 2010

Abstract

Drought is a complex natural hazard which is endemic to the Canadian Prairies. The 1999–2005 Canadian Prairie drought, which had great socio-economic impacts, was meteorologically unique in that it did not conform to traditional persistent ridging paradigms normally associated with Prairie drought. The purpose of this study is to diagnose the unique synoptic-scale mechanisms that lead to the subsidence in this drought. Using 30-day running means of percent of normal precipitation from station data, we identify key severe dry periods in 1999–2005. Analysis of the mean fields from reanalysis data shows that these dry events are associated with combinations of larger scale subsidence mechanisms of anticyclonic vorticity advection and cold air advection, along with the smaller scale subsidence mechanism of downslope flow. A brief historical perspective shows that the drought was centred in 2001–2002 and was not as severe as historical droughts, suggesting the increased vulnerability of society.

Résumé

La sécheresse est un désastre naturel qui est endémique aux Prairies canadiennes. La sécheresse canadienne de 1999–2005, qui avait alors eu de grands impacts socio-économiques, était météorologiquement unique car il n'était pas conforme aux paradigmes buttage persistants traditionnellement associés à la sécheresse des Prairies. Le but de cette étude était de diagnostiquer les mécanismes uniques à l'échelle synoptique qui ont conduit à la subsidence de cette sécheresse. En utilisant les moyennes glissantes de 30 jours des données de précipitation en pourcentage de la norme, nous identifions des périodes clés de sécheresse sévère entre 1999 et 2005. Analyse des champs moyennés des données de ré-analyse de ces périodes montre que ces évènements secs sont associés à des combinaisons de mécanismes de subsidence d'advection de tourbillon anticyclonique et d'air froid, ainsi qu'au mécanisme en plus petite échelle de descente d'air subsident. Une brève étude de l'histoire démontre que la sécheresse a été centrée entre 2001 et 2002, et n'était pas aussi sévère que les précédantes sécheresses historiques, suggérant que la vulnérabilités de la société a augmenté.

Acknowledgements

This research has been supported by Canadian Foundation for Climate and Atmospheric Sciences, NSERC, DRI, and Dr. Richard H. Tomlinson. I would like to acknowledge Éva Mekis (Environment Canada) for the corrected Canadian precipitation dataset, and ESRL PSD for freely providing the reanalysis, gridded precipitation, teleconnection index, and drought index data used in this study.

These two years in Montréal and this thesis would not have been possible without the love, support, patience, and guidance of many. Thank you, John Gyakum, for your patient guidance, willingness to help at any time, and genuine concern for your students and their well-being. Eyad Atallah and Shawn Milrad, thank you for the detailed research support and helpful thesis edits and comments. Gina Ressler, my dearest friend and fellow University of Alberta alumna, thank you for the cherished times we shared together in Montréal. Most of all, I would like to thank my family – Mom, Dad, Aaron, and Anna, as well as Garry, Diane, and John-Boy Hahn – upon whose shoulders I stand and to whom this thesis is dedicated. Words alone cannot describe my appreciation for everything you all have done for me – you all mean the world to me. Aaron, thank you specifically for your LaTeX mastery and the graduate school advice. Garry and Diane, thank you for welcoming and accepting me with open arms. Mom and Dad, I would not have been able to complete this without your understanding, gentle encouragement, and unconditional love and support. Lastly, to my other half, John-Boy, for your constant love and help in so many ways – editing, formatting, translation, patience, and motivation – throughout the completion of this thesis.

Contents

List of Figures

List of Tables

CHAPTER 1

Introduction

1.1 Motivation

1.1.1 Drought and Society

In many areas of the world, drought is a dreaded yet inevitable part of life, bearing largely negative impacts not only on agriculture, but on all of society. These negative impacts cover a very wide spectrum, depending on the severity of the natural drought event and the vulnerability of the targeted society. In developing nations that are prone to drought, such as those in Africa, society's vulnerability to drought impacts tends to be very high, owing to a combination of an undiversified economy, mismanagement of resources, and lack of political structure or will to mitigate drought. When highly vulnerable societies experience severe drought, the impacts are catastrophic. Not only can there be total crop failure and acute lack of clean water, but ultimately, drought can lead to food crises, famine, widespread malnutrition, increased spread of disease, and escalated mortality, particularly if there is political unwillingness to provide, or even accept, aid (e.g. 1998 drought/famine in Sudan) (Wilhite and Buchanan-Smith 2005). Drought can even induce conflict and increase political instability in these situations.

However, in developed nations with diversified economies, such as the United States (US) and Canada, the impact of drought on society manifests itself on less cataclysmic scales, due in part to the lower vulnerability of these nations. Nevertheless, the impacts of drought on these developed societies continue to be substantive. One of the main impacts drought has on developed nations is in the form of economic loss (i.e. decrease of Gross Domestic Product, GDP), owing to the negative impact on agriculture. The loss of GDP by agriculture is brought about by such factors as reduced crop yields, increased production/irrigation costs, decreased exports and increased imports of food products. In fact, drought exceeded hurricanes as the costliest weather disaster in the US from 1980–2003 (i.e. not including Hurricane Katrina in 2005), causing a total of $144 billion[1] in damages, according to the National Climatic Data Center's (NCDC) report on Billion Dollar Weather Disasters (Ross and Lott 2003). The droughts of 1980 and 1988 even topped the single weather event damage at $48.4 billion and $61.6 billion, respectively (Ross and Lott 2003). When drought is severe enough to put a strain on water resources, all aspects of society are affected. Industries that are directly affected by drought-induced water strain other than agriculture include forestry, fisheries, recreation/tourism, transportation and hydroelectricity (Maybank et al. 1995; Bonsal 2008). Drought can also lead to a rise in unemployment in a variety of sectors, and municipalities will often enforce limits on residential and commercial water usage in such conditions. The natural environment also cannot escape the damaging impacts of drought; much forest can be destroyed through increased numbers of wildfires, nutrient-rich top soils are often eroded by dust storms, and populations of ducks and other waterfowl decrease as the ponds and sloughs of their natural habitat desiccate. Water allocation and rights also become an increased issue during a drought and can lead to political tensions when water allocation is changed or promised amounts of hydroelectricity cannot be produced. This is a problem in many areas, such as California and Mexico, but is less of an issue in water-rich nations such as Canada.

[1] Adjusted to 2002 values.

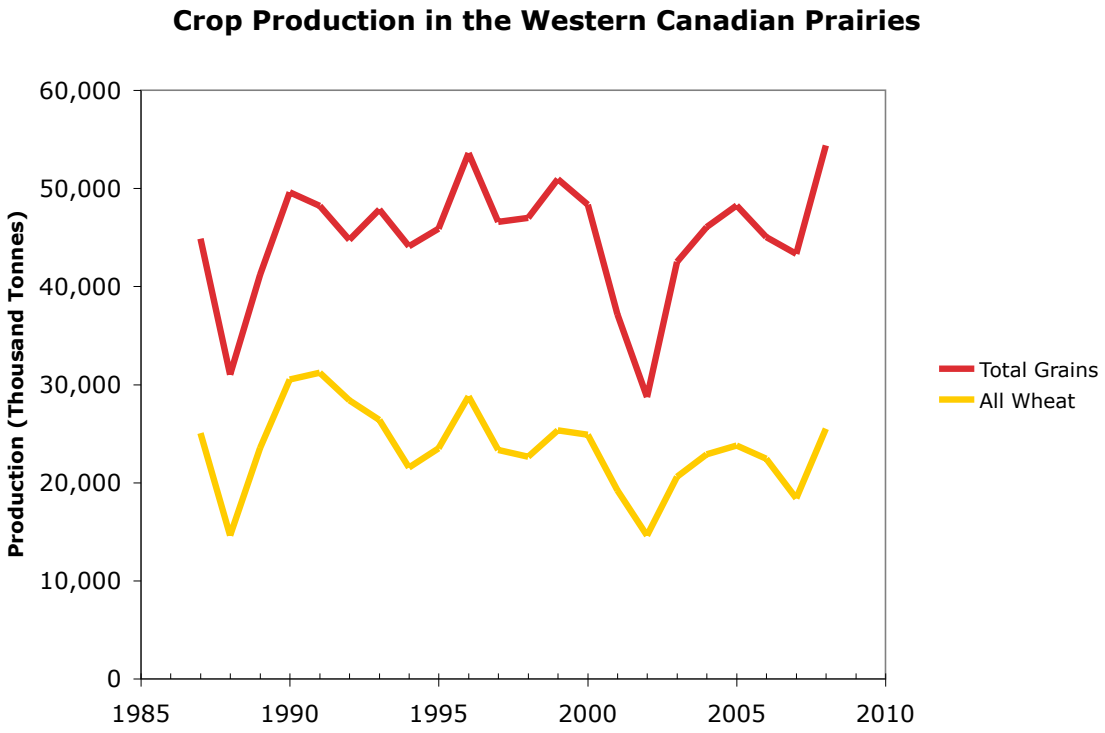

Figure 1.1: Crop production in the Western Canadian Prairies, 1987–2008. Total grains include wheat, durum, oats, barley, rye, flaxseed, and canola, and the All Wheat category is comprised of durum and wheat. Values are from Canadian Wheat Board Annual Reports of 1995–1996, 2000–2001, and 2007–2008 (Canadian Wheat Board cited 2010a, cited 2010b, cited 2010c).

In Canada, drought is endemic to, and a frequent concern in the agriculture-dominated Prairie provinces, where there have been no less than 40 drought occurrences in the last 200 years (Nkemdirim and Weber 1999; Maybank et al. 1995; Bonsal 2008; Phillips 1990). Extensive and multi-year droughts have occurred in the Canadian Prairies in the 1890s, 1930s (the "Dirty Thirties"), 1960s (with 1961 as the worst single-year drought), the 1980s, and most recently, in 1999–2005 (Bonsal and Wheaton 2005; Bonsal 2008; Chipanshi et al. 2006; Maybank et al. 1995; Phillips 1990). The sectors which take the hardest hit are agriculture and water resources, but other industries, as mentioned above (e.g. forestry), are affected as well. Figure 1.1, a plot of grain production in the Western Canadian Prairies from 1987–2008, plainly demonstrates the devastating impact of drought on agriculture in the Prairies. Dramatic drops in production are seen in 1988, corresponding to the 1980s drought, and also in 2002, corresponding to the most recent 1999–2005

drought.

The recent Canadian Prairie drought of 1999–2005 has been called "the worst drought for at least a hundred years" in terms of socioeconomic impact (Bonsal 2008). Economic and agricultural impacts were staggering, amounting to a $5.8 billion drop in GDP and a loss of 41 000 jobs in 2001–2002, and ultimately leading to the first occurrence of negative net farm incomes in over 25 years (Bonsal 2008; Wheaton et al. 2008). Outbreaks of grasshoppers occurred, adding to crop damage, and Albertan cattle numbers decreased by 600 000 (10%) in 2002 (Wheaton et al. 2008). River and stream flow in Alberta and Saskatchewan was extremely below average (and in some cases nonexistent) from 2000–2003 (Wheaton et al. 2008). In addition, the amount of natural Prairie ponds reached an all-time low in May 2002 (Wheaton et al. 2008). This drought also caused greatly increased amounts of forest fires in Alberta in 2002, and hindered the generation of hydroelectricity in Manitoba and British Columbia (Bonsal 2008; Wheaton et al. 2008).

In fact, drought was not restricted to the Prairies during this time period. Drought conditions were felt coast-to-coast across Canada in 2001–2002, and plagued many areas across the globe (e.g. US, Southern Europe, and Southwest to Central Asia) (Bonsal 2008; Hoerling and Kumar 2003). These conditions have been ongoing since 1999 in Western US, provoking it to be named the "turn of the century" drought[2] (Cook et al. 2010). In Canada, regions of Central Alberta in the vicinity of Edmonton have most recently experienced drought conditions in 2009–2010 (see North American Drought Monitor, http://ncdc.noaa.gov/nadm.html, which shows regions of Central Alberta being under Extreme Drought (D3) from June 2009 to March 2010 inclusive).

This "turn of the century," or perhaps more aptly, "turn of the millennium" drought has spawned additional research into the causes of drought (e.g. Hoerling and Kumar 2003; Cook et al. 2010; Seager 2007) and some research network initiatives (e.g. Drought Research Initiative in Canada). This momentum for drought re-

[2]It is important to elucidate that a 10-year drought does not imply a 10-year void of precipitation events.

search is likely to continue, including mitigation and adaptation strategies, particularly in light of two consequential concepts – the ever increasing world population and perhaps most importantly, climate change. The increase in need for clean water and food to match the rising population inevitably leads to more water and land stress, thus increasing society's vulnerability to drought regardless of the severity of the natural drought event. What is perhaps more disconcerting are the results from the Fourth Assessment Report of the Intergovernmental Panel on Climate Change (IPCC). The IPCC notes that spatial coverage of drought has expanded in the past three decades (Trenberth et al. 2007). In addition, IPCC modelling studies of future scenarios point to increased drying and poleward expansion of arid subtropical zones (Cook et al. 2010; Meehl et al. 2007). Thus, the probable intensification of societal drought impacts in the future, owing to increases in severity and vulnerability, should continue to fuel the crucial area of drought research.

1.1.2 Drought Dynamics: The recent 1999–2005 period

Not only was the 1999–2005 drought significant in terms of the socioeconomic impact, but it was also driven by meteorological conditions distinct from earlier droughts. This drought did not conform to the circulation patterns normally associated with Canadian Prairie drought, namely large-scale and persistently positive Pacific/North-American (PNA) -like (Wallace and Gutzler 1981) ridging or "blocking" over Western Canada, accompanied by anomalously warm temperatures (see Section 1.2.3 for further details), thereby challenging the validity of the traditional drought paradigm (Bonsal and Wheaton 2005; Bonsal 2008; Wheaton et al. 2008). Figure 1.2 shows the anomalous 500-hPa upper-level structure for the autumn to summer period for two historical Canadian Prairie drought periods, 1961 and 1988, in comparison with 2001 and 2002 (from Fig. 2 of Bonsal and Wheaton (2005)). It is clear from this figure that the classic positive PNA-like anomalous ridging in Western Canada and North Pacific troughing, which sets up anomalous meridional flow in Western Canada, occurred in 1961 and 1988 but not in 2001 and 2002. Alternatively, positive anomalies encompassed the North Pacific and most of North

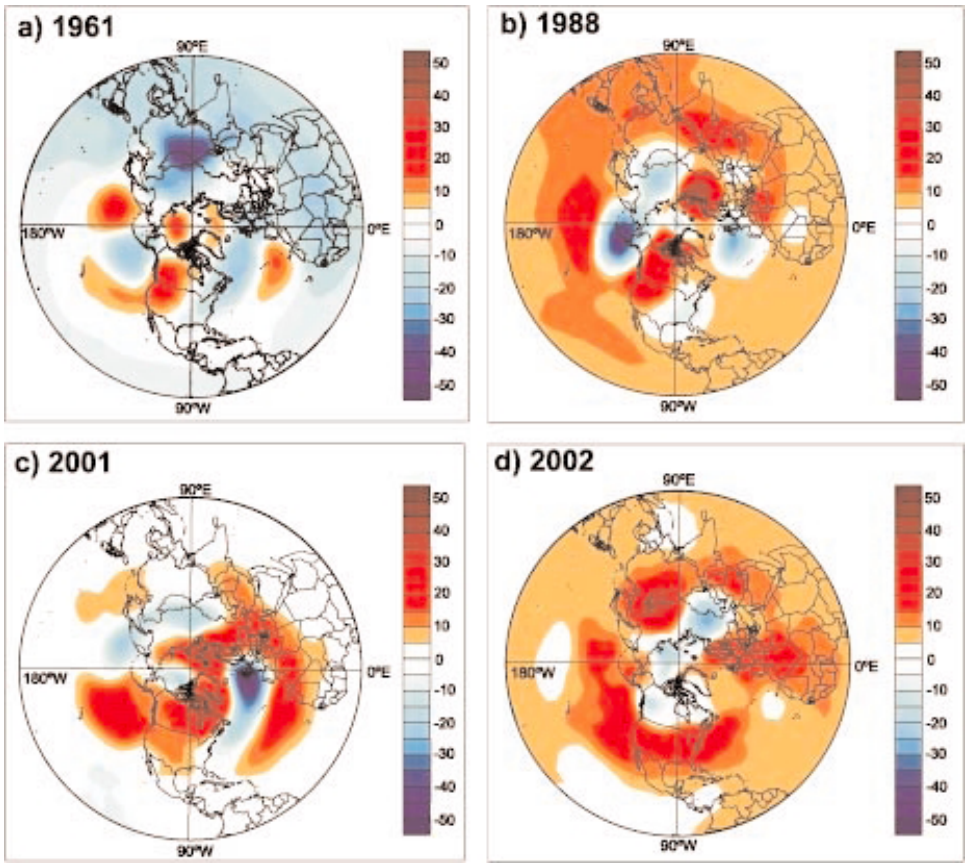

Figure 1.2: 500-hPa September to August anomalies (m) relative to 1948–2002 (NCEP/NCAR Reanalysis) for selected Canadian Prairie droughts. Taken from Fig. 2 of Bonsal and Wheaton (2005).

America in 2001 and 2002, with the anomalies being centred farther south in a zonal band structure over the US in 2002 (Bonsal and Wheaton 2005). Given the unique upper level patterns in 2001 and 2002, it is not surprising that the spatial structure for temperature and precipitation anomalies were also distinct from previous Canadian Prairie droughts. Bonsal and Wheaton (2005) showed that the negative precipitation anomalies for the 1961 and 1988 droughts were mostly confined to the extreme southern Prairies, and were accompanied with strong positive temperature anomalies in the 1.5–2.5 °C range. On the other hand, the precipitation deficits in 2001 and 2002 tended to be centred farther north, and the temperature anomalies were on average very weak (0.5–1 °C), both of which add to the unique character of this drought. In fact, the spring of 2002 was the coldest spring in the Prairies since 1948 (Bonsal and Wheaton 2005).

Another major aspect in which the 1999–2005 drought differed from previous Canadian Prairie droughts was the fact that there was no clear relationship to teleconnection patterns (i.e. no consistent or persistent teleconnection signal) (Bonsal 2008). Bonsal and Wheaton (2005) noted negative Pacific Decadal Oscillation (PDO) (Mantua et al. 1997), weak inconsistent PNA values, and La Niña conditions in 2000-01, followed by a period of neutral conditions and El Niño in 2002. This differed markedly from the strongly positive PDO and PNA in 1988 and 1961.

Therefore, because of the particularly significant economic impact and highly anomalous and interesting meteorology, we intend to study the specific dynamical mechanisms of the 1999–2005 Canadian Prairie drought.

1.2 Literature Review

1.2.1 Defining and Quantifying Drought

Drought truly resides in a class of its own compared to other extreme weather events because of its complexity. Descriptions of drought as a "creeping phenomena" (Wilhite and Buchanan-Smith 2005), a "catastrophic non-event" (Weber and Nkemdirim 1998), or as "quietly wreaking havoc" (American Meteorological Society 2004) attempt to capture the slow nature of its onset, maintenance, and cessation. As Tannehill (1947) fittingly describes it, "...we scarcely know a drought when we see one...we are not sure about it until the crops have withered and died." Because of its complex and elusive nature, merely defining drought, and simply determining when a drought begins or ends, are difficult tasks in themselves. This difficulty is compounded further in the attempt to measure or quantify drought. Part of what makes drought difficult to define and study is that every drought is unique, differing in (and thus can be characterized by) duration, spatial extent, and severity/intensity (Wilhite and Buchanan-Smith 2005). For instance, drought can occur on many different timescales – months, years, decades, or even centuries (the so-called "megadroughts") (Wilhite and Buchanan-Smith 2005). These character-

istics are, or attempt to be, embodied by what is known as a drought index; this is a synthesized, quantitatively-scaled version of meteorological and hydrological variables (Steinemann et al. 2005) or as defined by the AMS (American Meteorological Society cited 2010), "a computed value related to some of the cumulative effects of a prolonged and abnormal moisture deficiency." Quantifying drought through an index is appealing to meteorologists for ease of drought comparison, but is arguably more important in making drought simpler to understand for policy makers and the public who are directly affected (i.e. agriculturalists). Nevertheless, a disconnect often still exists between the public perception of drought and quantifying drought duration, severity, and spatial extent using drought indices.

What defines a drought is largely dependent on the local climatic characteristics of the affected region. For example, it would take a larger precipitation deficit for the effects of drought to be felt in a humid climate as opposed to a naturally arid climate. Historical definitions of drought reflected this fact that it was specific to each region (e.g. drought in England was 14 consecutive days that received less than 0.25 mm on each day (Tannehill 1947)). Having one way to define drought quantitatively using indices, or otherwise, is rather appealing, but the search for such an idealized "formula" has been the source of much debate and consternation. The fact remains that some drought indices succinctly and accurately describe drought in certain areas of the world, but fail at capturing it in other regions. For this reason, Wilhite and Buchanan-Smith (2005) suggests that "the search for a universal definition of drought is a rather pointless endeavour." Likewise, for drought indices, Heim (2002) asserts that "the considerable disagreement that exists about the definition of drought makes it impossible to devise a universal drought index." Nevertheless, there are four commonly accepted and generalized types of drought – meteorological or climatological, agricultural, hydrological, and socioeconomic and political drought – each accompanied by a collection of drought indices.

Meteorological or Climatological Drought:

This is loosely defined as an extended period of time with below-normal precipitation, i.e. the first natural event, and the foundation for the other drought types (Wilhite and Buchanan-Smith 2005). Alternatively, Heim (2002) describes it as "the atmospheric conditions resulting in the absence or reduction of precipitation." It is important to note that meteorological drought does not imply an absolute nonexistence of any precipitation for the entire drought period – it is the cumulative long-term effect which is most important.

There are many meteorological drought indices, all of which are based on climatological fields such as of precipitation, temperature, evapotranspiration, or a combination of such variables (Steinemann et al. 2005). The most common are as follows:

- Percentage of normal: This is one of the most straightforward indicators of meteorological drought – a simple ratio of the current accumulation (usually for a month) with the climatological, or normal, value.

  Limitations: Precipitation is not a normally distributed variable; rather, it is positively skewed, where the median is less than the mean. This translates to below-normal precipitation being more probable than above-normal precipitation. Some arguments against this technique include the fact that the same percentage does not hold the same meaning at different locations, and the difficulty in associating the percentage with a societal impact (Steinemann et al. 2005).

- Palmer Drought Severity Index, PDSI: The PDSI, meant as a meteorological drought index, has values ranging from below -4 (Extreme drought) to above 4 (Extremely wet) as seen in Table 1.1, and is calculated using temperature and precipitation data in the method as follows (Palmer 1965):

  First, what is known as the normalized, or Climactically Appropriate for Existing Conditions (CAFEC) Precipitation, $\hat{P}$, is computed in a moisture/water

Table 1.1: PDSI categories (Palmer 1965)

Moisture Class	PDSI
Extremely Wet	≥ 4.00
Very Wet	3.00 to 3.99
Moderately wet	2.00 to 2.99
Slightly wet	1.00 to 1.99
Incipient wet spell	0.50 to 0.99
Near normal	0.49 to -0.49
Incipient drought	-0.50 to -0.99
Mild drought	-1.00 to -1.99
Moderate drought	-2.00 to -2.99
Severe drought	-3.00 to -3.99
Extreme drought	≤ -4.00

balance equation:

$$\hat{P} = \hat{ET} + \hat{R} + \hat{RO} - \hat{L} \tag{1.1}$$

where $\hat{ET}$, $\hat{R}$, $\hat{RO}$, and $\hat{L}$ are the CAFEC quantities for evapotranspiration, recharge, runoff, and loss, respectively. Next, an intermediary quantity known as the Palmer Z-index (or the moisture anomaly index) is calculated:

$$Z = (P - \hat{P})K \tag{1.2}$$

where P is the areal averaged precipitation, and K is the local climatic characteristic, or weighting factor (empirical). Finally, the PDSI for each month, $PDSI_i$, is calculated in the following method:

$$PDSI_i = 0.897 PDSI_{i-1} + \frac{Z_i}{3} \tag{1.3}$$

The PDSI value for a month is thus dependent on 2 factors, the PDSI value of the previous month, $PDSI_{i-1}$, giving it long term memory, and the Palmer Z-index. Despite being meant as a meteorological drought indicator, the PDSI tends to be best in phase with agricultural impacts (Heim 2002). The Z-index has a much shorter memory than the PDSI, and is also used as a separate index itself. In fact, Quiring and Papkryiakou (2003) concluded that Palmer's Z-index was the best indicator of agricultural drought in the Canadian Prairies; the Z-index had the highest correlation, and lowest root mean

square and mean absolute error to Canada Western Red Spring wheat yield, as compared with three other indices.

Limitations: There are several arguments against the PDSI, mainly involving the limited two-layer soil moisture model (Heim 2002). The PDSI does not consider snow cover, snow melt or frozen ground, leading to its limited utility during cold seasons at mid- to high latitudes (Dai et al. 2004; Heim 2002). Another main argument is that the PDSI is spatially variant, meaning that a single PDSI value does not have the same qualitative value at all locations. This stems from the fact that the the empirical constants in the equation for the weighting factor, K, were scaled using data from only nine climate divisions in the US Great Plains (Heim 2002).

- Standardized Precipitation Index, SPI: Created by McKee et al. (1993), the SPI uses only precipitation data, and resembles a spatial comparison of the standard deviation of precipitation. In the SPI calculation, the probability distribution of precipitation is computed by fitting historical records of precipitation at different timescales to a Gamma function (Pearson Type III), and then normalising to give a mean of zero and standard deviation equal to one. SPI values are similar to PDSI, in that negative values indicate dry conditions, and positive values indicate wet conditions (see Table 1.2). The main benefit of SPI is that it is spatially invariant, and thus comparable amongst all locations (McKee et al. 1993; Heim 2002). Interestingly, the World Meteorological Organization (WMO) recently declared in the "Lincoln Declaration on Drought Indices" that the SPI should be used as a universal drought index for meteorological drought (World Meteorological Organization cited 2010).

Table 1.2: SPI categories (McKee et al. 1993)

Drought Category	**SPI**
Mild drought	0 to -0.99
Moderate drought	-1.00 to -1.49
Severe drought	-1.50 to -1.99
Extreme drought	≤ -2.00

Limitations: Precipitation measurements are not as reliable in the winter, owing to turbulent wind effects and wetting losses (Groisman and Legates 1994). In addition, since temperature is not included in the SPI calculation, it may be more difficult to quantify the effects of warming under anthropogenic climate change on drought distribution and intensity.

Agricultural Drought:

Agricultural drought deals with deficiencies in soil moisture, particularly in the root zone (surface layer), to the point where it severely hinders crop growth. In agricultural regions that are predominantly dependent on precipitation as the source of soil moisture, as opposed to irrigation, agricultural drought is a lagged result of its meteorological counterpart. In regions that are more irrigation dependent, agricultural drought is additionally lagged and more related to the levels of surface and subsurface water (hydrological drought). Agricultural drought also depends on temperature, previous soil conditions, soil type, vegetation or crop type, evapotranspiration, and infiltration (Wilhite and Buchanan-Smith 2005; American Meteorological Society 2004; Heim 2002).

A few agricultural drought indices are as follows:

- Crop Moisture Index, CMI: This is Palmer's agricultural drought index, which stems from the PDSI. It depends on precipitation and temperature data like the PDSI; however, it is calculated on a weekly basis and is not meant as a long-term drought indicator as it changes rapidly according to the available moisture (Heim 2002; Hayes cited 2010).

- Satellite-Based vegetation indices: There are a number of remotely sensed vegetation or crop indices which use radiance data from the Advanced Very High Resolution Radiometer (AVHRR). These include the Vegetation Condition Index (VCI), and the more widely used Normalized Difference Vegetation Index (NDVI), which is represented by the relation (American Meteorological

Society cited 2010):

$$NDVI = \frac{NIR - RED}{NIR + RED} \tag{1.4}$$

where *NIR* and *RED* are respectively the measured near-infrared and red radiances. These indices allow for real-time drought monitoring, but are normally only functional during the growing season, as they are vegetation-based (Heim 2002).

Hydrological Drought:

Hydrological drought is related to the decrease in surface and subsurface water levels (e.g. groundwater, lakes, aquifers, reservoirs). This is normally a delayed effect of meteorological drought, and typically has a prolonged recovery period, owing to the slow nature and recharge of the hydrologic system. The timeliness of the response of the hydrological system to meteorological drought, however, is ultimately dependent upon the specific characteristics of the hydrologic basin in question (i.e. size and composition of the basin), and thus the response and recovery time can vary from basin to basin. Nevertheless, hydrological drought typically still exists after precipitation amounts return to normal. Hydrological drought is also affected by a large range of human activities, such as recreation, irrigation, and hydroelectricity production. The severity of the impacts can also be heightened by poor and inflexible water management practices (Wilhite and Buchanan-Smith 2005; American Meteorological Society 2004; Heim 2002).

Hydrological drought indices are based off of hydrological system variables such as streamflows, snow pack, and levels of groundwater, lakes, and ponds (Steinemann et al. 2005). These include the Palmer Hydrological Drought Index (essentially a longer term PDSI), and the Surface Water Supply Index (SWSI), a modified PDSI which attempts to take into account snowpack and high elevation precipitation (Heim 2002).

Socioeconomic and Political Drought:

This type of drought deals with the impacts that the above natural events (meteorological, agricultural, and hydrological) have on society, development, economics, and political activity. It encompasses impacts such as the supply and demand of precipitation-reliant commodities (i.e. hydroelectricity), but also includes extreme cases where violent conflict arises between groups of people who are affected differently by drought (e.g. nomadic vs. settled farmers/grazers in Africa) (Wilhite and Buchanan-Smith 2005). There is no "real" computed index for this type of drought. However, one can argue that there is no need for such a quantification, as societal impacts, such as those mentioned in Section 1.1.1, are sufficiently apparent as is (e.g. value of GDP loss).

Given the strengths and limitations of the collection of drought indices, perhaps the "best" index is not one, but in fact a collaborative display of many indices. This idea has been put to use in the creation of the Drought Monitor, available for the US, since 1999, and North America, since 2002 (Heim 2002).

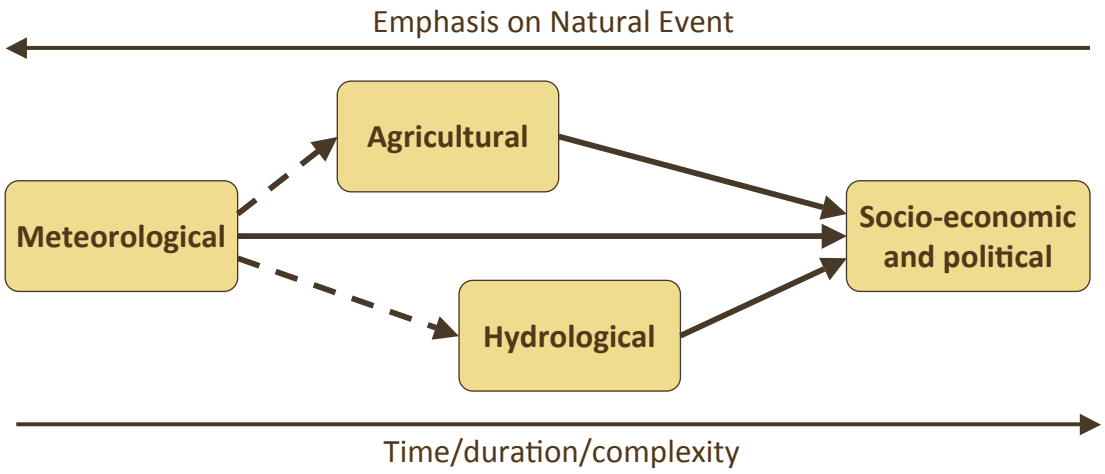

Figure 1.3: Relationships between drought types. Adapted from Fig. 1 of Wilhite and Buchanan-Smith (2005)

These four types of drought are deeply intertwined and are dependent on each other, where meteorological drought is the catalyst for the other types of drought. The "break-off" drought types are increasingly complex compared to meteorolog-

ical drought, and have decreasing relation to the natural event. Figure 1.3 is a depiction of this relationship. The dashed arrows in Fig. 1.3 represent the ideas that meteorological drought does not always lead to agricultural and hydrological drought, and the fact that agricultural drought can occur without hydrological drought, and vice versa. For example, a lack of precipitation may occur when it is not essential for crop growth, not affecting agriculture, but having an impact on lake and ground water levels. All three natural events undoubtedly impact society.

The complete study of any drought requires an in-depth look at both the meteorology and the agricultural-social-political state at the time. However, such a study is beyond the scope of this thesis, and thus, only the meteorological drought will be considered henceforth.

1.2.2 The Canadian Prairies – Meteorology, topography, and vulnerability

Figure 1.4: Palliser's Triangle, from the Encyclopedia of Saskatchewan (Dale-Burnett cited 2010).

The Canadian Prairie provinces of Alberta, Saskatchewan, and Manitoba contain more than 80% of Canada's crop and range land (Chipanshi et al. 2006). The prairie ecozone itself is located in the southern parts of these provinces, covering approximately 520 000 km^2 (Quiring and Papkryiakou 2003), and encompasses an area known as Palliser's Triangle (Fig. 1.4), one of the driest regions in Canada. This region was initially described by 19th century British explorer Captain John Palliser as "desert or semi-desert like in character, which can never be expected to become occupied by settlers" and was determined to be poorly suited for farming (Dale-Burnett cited 2010).

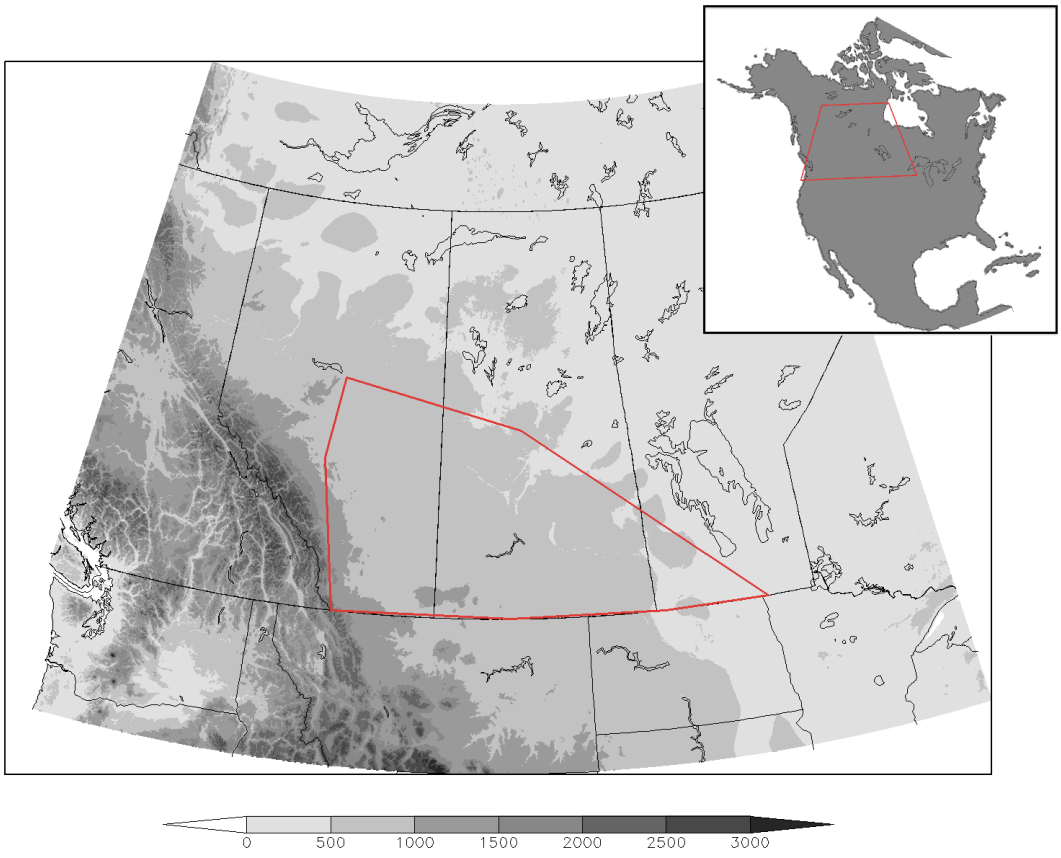

Figure 1.5: Elevation of Western Canada, ETOPO1 dataset (Amante and Eakins 2009). The units of elevation are in m. The area outlined in red is the approximate extent of the study area.

Part of what makes the Prairies prone to drought is the fact that they reside on the lee side of the Rocky Mountain Range in the rain shadow region (Fig. 1.5). The Rockies act as a barrier for Pacific moisture, where westerly trajectories off the

ocean are depleted of their moisture through orographically forced precipitation on the West Coast. The Prairies are also far removed from large moisture sources. In fact, the two main moisture sources for the Canadian Prairies are the Gulf of Mexico and the Pacific Ocean, with the Gulf being the most important for summer precipitation, and the Pacific for winter precipitation (Liu et al. 2004).

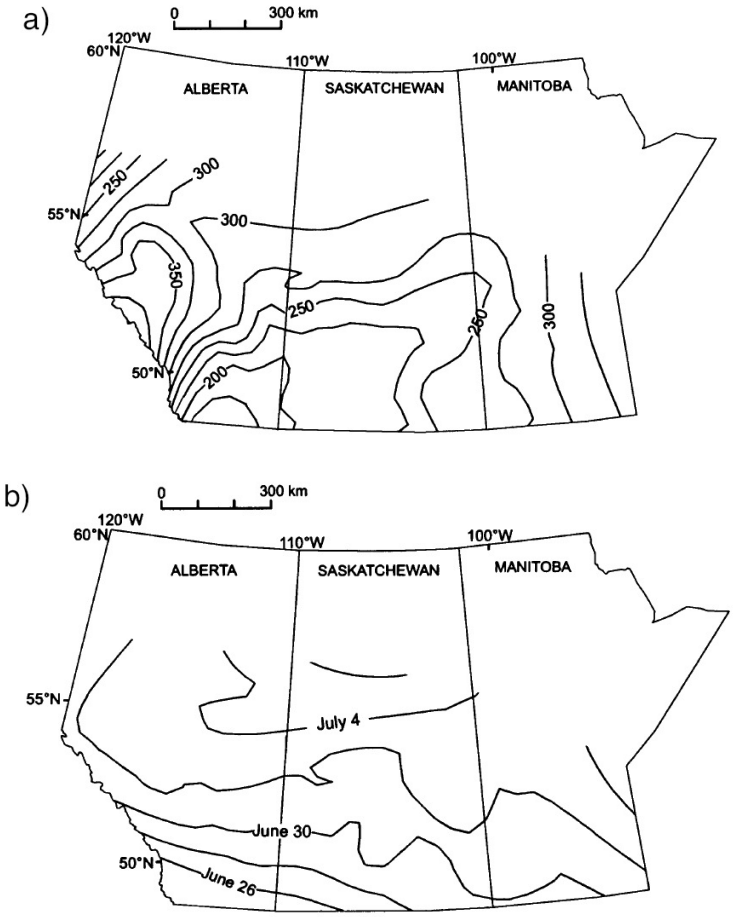

Figure 1.6: a) Canadian Prairie growing season precipitation accumulation (mm), 1961–90 average. Taken from Fig. 2 of Bonsal et al. (1999). b) Date of maximum precipitation, 1961–90 average. Taken from Fig. 4 of Bonsal et al. (1999)

Another factor that adds to the susceptibility of the Prairies to drought is the high temporal and spatial variability of precipitation (Bonsal and Wheaton 2005; Maybank et al. 1995). In other words, precipitation amounts vary from season to season. Up to two-thirds of the annual total of precipitation in the Prairies falls in the growing season (May to August) (Bonsal et al. 1999; Dey 1982). Growing

season precipitation amounts vary across the Canadian Prairies, with a minimum of less than 200 mm in southern Alberta, gradually increasing eastward to 300 mm in Manitoba and northwestward to greater than 350mm along the Rocky Mountains (Fig. 1.6a). These amounts are "just enough...to sustain agriculture" (Bonsal et al. 1999), thus any departure from these values, no matter how small, could potentially hinder crop growth. The Canadian Prairies receive the greatest amount of precipitation in late June to early July, which conveniently coincides with the greatest water demand for crop growth (Bonsal et al. 1999). The date of maximum precipitation varies spatially from the end of June in southern Alberta, to early July farther north (Fig. 1.6b), following the seasonal migration of the jet stream as seen in the seasonal surface climatology in Fig. 1.7. The fact that the growing season is the period of maximum precipitation in the Prairies is exemplified in Fig. 1.7c, the summer (June-July-August, JJA) surface climatology. The dominant high pressure system located off of the West Coast, drives the 1000–500 hPa thickness trough upstream of the Prairies, a position that is conducive to ascent. The geostrophic surface wind in summer is also ideal for moisture transport from the Gulf of Mexico into the Prairies, providing the needed moisture for precipitation. This contrasts with winter (December-January-February, DJF) in Fig. 1.7a in which the strong Gulf of Alaska low and a continental high in the US block moisture transport form the Gulf of Mexico. Although the amount of cold season precipitation is relatively minor compared to the growing season, drought conditions can be aggravated by low snow cover.

Not only is the amount of growing season precipitation important for drought occurrence, but also the timing of it, according to crop need. For example, the growing season of 1988 received a normal amount of precipitation, but mostly fell in August, too late for crop growth (Bonsal et al. 1999). This was also the case for some areas in Alberta and Saskatchewan in summer of 2002 (Wheaton et al. 2008). Thus, even if a certain growing season may not appear meteorologically significant in terms of negative precipitation anomalies, the temporal distribution needs to be considered in order to link it to agricultural and socioeconomic drought. Drought

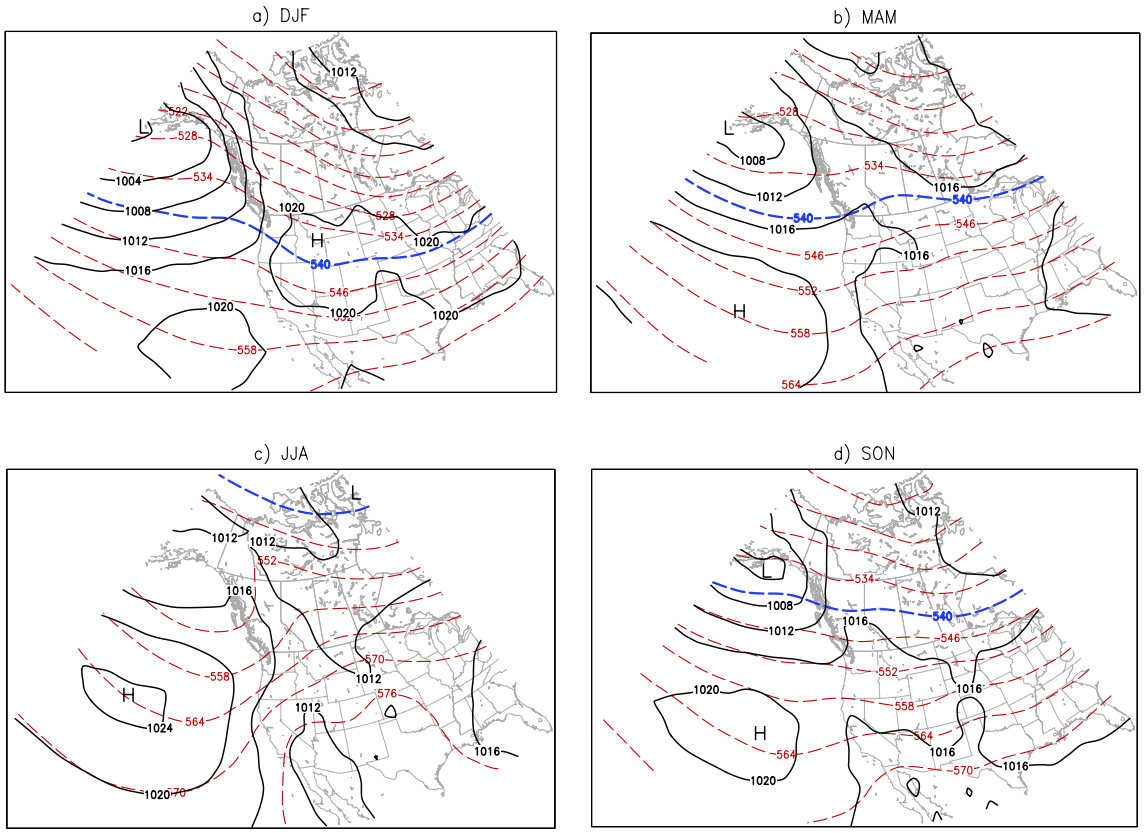

Figure 1.7: MSLP (solid, 4 hPa interval) and 1000–500 hPa thickness (red dashed, 6 dam interval) climatology (1979–2008) for a) DJF, b) MAM, c) JJA, and d) SON from the NCEP-NCAR Global Reanalysis. The 540 dam thickness contour is emboldened in blue.

conditions in the Prairies are also intensified by high temperatures.

1.2.3 Prairie Drought Dynamics

Using instrumental PDSI, Cook et al. (2010) found that the recent 2000s drought was *not* unprecedented for the US (i.e. was not as intense) compared to the two most severe droughts in the 20th century, notably the 1930s and 1950s for the US. In the context of a much longer paleoclimate record, however, even these two 20th century droughts are rather unremarkable compared to "megadroughts" of the Medieval Warm Period (900–1300AD) (Cook et al. 2010). These megadroughts are identified in western US and in the Mississippi Valley by reconstructed PDSI from tree-ring records in Cook et al. (2010). However, in a tree-ring reconstruction for the

Canadian Prairies, St. George et al. (2009) suggest that "there is no regional analog" in Canada to the US and Mexico megadroughts of the 16th century. It remains clear from both the tree-ring record in St. George et al. (2009) and PDSI and SPI instrumental records (Bonsal and Regier 2007) that the recent 1999–2005 Canadian Prairie drought pales in comparison with early 20th century droughts (1930s). Part of the "shock," or perceived extreme severity, of the 1999–2005 drought arose from the fact that it followed an anomalously wet period, or an absence of dry conditions in the 1990s (Bonsal and Regier 2007; Wheaton et al. 2008).

In terms of multi-decadal causes of drought, McCabe et al. (2004) provided very convincing evidence relating drought in the US to the PDO and the Atlantic Multidecadal Oscillation (AMO) (Kerr 2000). Using a rotated principal components analysis of the timeseries of drought frequency, McCabe et al. (2004) found that the first and second leading components were temporally and spatially correlated very strongly, and significantly with the PDO and AMO, respectively. McCabe et al. (2004) indicate that positive AMO brings about widespread drought in the US, regardless of the PDO phase, with the 1998–2002 US drought being under a positive AMO and negative PDO regime. McCabe et al. (2004) found that the correlation of any of the components with the NINO3.4 Index was smaller and less significant. This fact is surprising, and rather contradictory to the findings of many other studies that largely point to La Niña as the instigator of drought in North America (Cook et al. 2010; Karnauskas et al. 2008; Seager 2007; Hoerling and Kumar 2003). These studies, however, mostly focus on drought in the US. There were persistent warm sea surface temperature (SST) anomalies in the Western tropical Pacific and persistent cold SST anomalies in the Eastern tropical Pacific (i.e. La Niña-like conditions) during 1999–2005 (Hoerling and Kumar 2003). General Circulation Models (GCMs) forced by such SST signatures reproduced anomalous temperature and precipitation patterns similar to observations over the Northern Hemisphere lower mid-latitudes in 1999–2005 (e.g. US). However, the GCMs lacked adequate representation of the polar latitudes (i.e. Canada), particularly in upper height anomalies, and thus it was suggested that the oceans may not be the main forcing for the

drought in the higher latitudes (Hoerling and Kumar 2003).

These findings regarding La Niña and North American drought patterns are largely in conflict with studies that specifically focus on the Canadian precipitation patterns and drought in the Canadian Prairies. In a study of the response of Canadian precipitation to El Niño-Southern Oscillation (ENSO), Shabbar et al. (1997) found that in general, El Niño resulted in anomalously dry conditions across southern Canada, including the Prairies, in the winter after onset. On the other hand, wetter than normal conditions occurred in the winter after La Niña onset. The dry (wet) conditions are explained by positive (negative) PNA-like patterns. This is related to the idea shown in studies that a large degree of the variance of PNA is explained by ENSO (e.g. Shukla et al. 2000). It is interesting to note that the driest 10% of January-February-March (JFM) in Shabbar et al. (1997) do not include the 1961 and 1988 Canadian Prairie droughts, shedding importance on growing season precipitation as opposed to winter precipitation with regards to Prairie drought. Shabbar and Skinner (2004) supported these results and provide a link to Prairie drought by using singular value decomposition (SVD) of winter SST patterns and the subsequent summer PDSI values. The second and third modes (48% of the squared covariance) were associated with ENSO and PDO, and were termed as the "most significant processes in drought variability" (Shabbar and Skinner 2004). Again, the general conclusion was that drought in Western Canada, as defined by negative PDSI values in the summer, follows an El Niño (positive PNA) event (Shabbar and Skinner 2004).

The study by Bonsal and Chakravarti (1993) on the connection between SST anomalies in the North Pacific and dry spells during the Canadian Prairie growing season concluded that the probability of a dry spell increases as the duration of a positive SST anomaly gradient in the North Pacific (i.e. warm anomalies off the coast of British Columbia and cold anomalies in the central North Pacific, see Fig. 1.8) increases. Bonsal and Chakravarti (1993) gave a 100% probability of growing season dry spell occurrence when these anomaly gradients persist for more than nine months. However, this study defined dry spells with a necessary criteria of

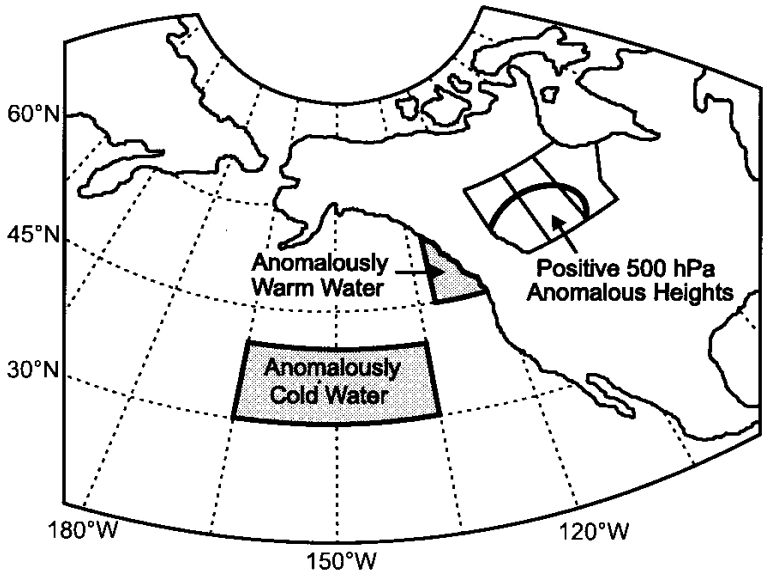

Figure 1.8: North Pacific SST and 500-hPa anomalies that correspond to Canadian Prairies dry spells. Taken from Fig. 1 of Bonsal and Lawford (1999).

positive 500-hPa height anomalies (ridging), therefore limiting the correlation to dry conditions only associated with persistent ridging. Thus, the fact that Canadian Prairie drought can be caused by mechanisms other than ridging was inherently disregarded in this study. The arguments in Bonsal and Chakravarti (1993) are expanded to include ENSO in Bonsal and Lawford (1999), in which it is found that more extended dry spells occur in the Canadian Prairies in the second summer after the onset of an El Niño event, and less dry spells occur in the second summer following a La Niña event. However, it was noted that El Niño dry spells (and positive 500-hPa anomalies) occurred without persistent North Pacific SST gradients (e.g. 1951, 1969 El Niño), but also that some dry spells with positive SST gradients (e.g. 1961) were not associated with El Niños. It was concluded in (Bonsal and Lawford 1999) that El Niño and La Niña events: a) were not necessary to produce dry spells in the Canadian Prairies, and b) had a more significant impact on precipitation frequency, rather than precipitation amounts. At best, this study only indicates that there are associations between ENSO, PNA, 500-hPa heights, and consecutive dry days on the Prairies.

The small number of studies that have investigated the dynamical causes of

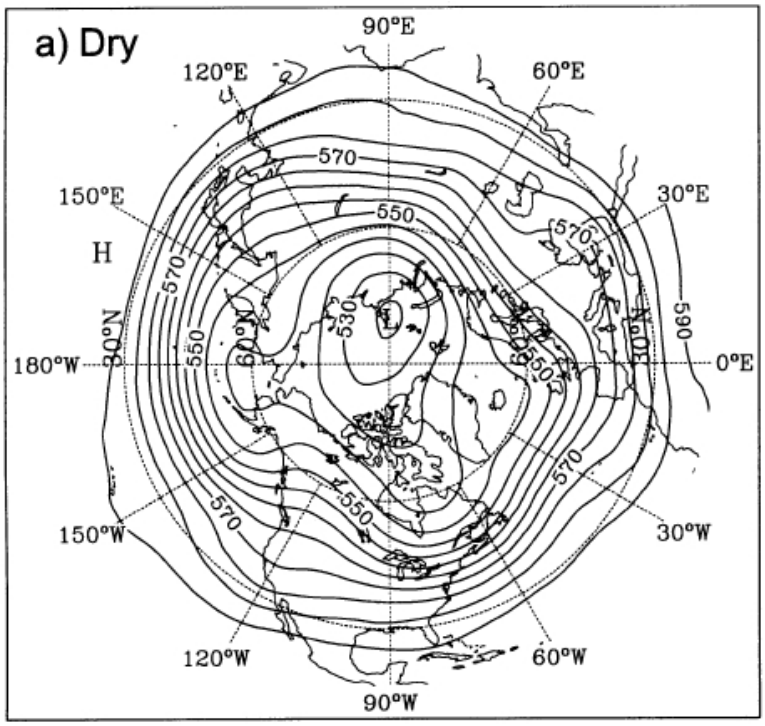

Figure 1.9: Composite 500-hPa circulation for five driest Mays between 1946–1996. Taken from Fig. 8a of Bonsal et al. (1999).

drought in the Canadian Prairies have conclusions mainly restricted to persistent ridging caused by PNA-like patterns. Based on the two driest summers between 1941 and 1970 (i.e. 1961 and 1967), Dey (1982) determined that the dominant dynamic mechanism of Canadian Prairie drought was a quasi-stationary mid-tropospheric ridge over Western Canada, accompanied by a downstream northwest-southeast jet. In this case, the blocking causes systems and associated moisture to be displaced north of the Prairies. These findings are supported by those in Knox and Lawford (1990) and in Bonsal et al. (1999), whose 500-hPa composites of the five driest Mays between 1946 and 1996 show anomalous ridging over western North America, and anomalous troughing over eastern North America (see Fig. 1.9), giving rise to meridional flow over the continent. In this set up, the ridge axis is slightly west of the Prairies, and is the mechanism for subsidence and diversion of systems northward. This 500-hPa pattern was "most pronounced" in May and June, as opposed to July. Bonsal et al. (1999) extended his study to mean sea level

pressure (MSLP) composites, and determined that growing season precipitation in the Canadian Prairies is influenced by the interplay of the strength and position of three main surface features – a low over south-western continental US (CONUS), an Arctic high, and a low over eastern Canada. Dry conditions occurred with a weak, southward displaced CONUS low and westward displaced Arctic high and Canadian low.

In terms of western North American ridging, it is interesting to note that intense water vapour transport (IWVT) events into the high latitudes of western North America ("pineapple express") during the cool season have been shown to intensify ridging in western North America through enhanced diabatic heating (Roberge et al. 2009). These events can in fact enhance drought conditions over the Prairies; a warm 1000–500 hPa thickness anomaly of over 120 m, or 6 °C, occurred in a composite of 11 winter IWVT events during 1999–2004.

1.3 Purpose

As stated above, previous literature only provides, at best, associations or correlations between large-scale seasonal patterns and drought occurrence in the Canadian Prairies. It is critical, however, to look on a finer timescale than seasonal averages because the highly variable nature of precipitation on the Prairies is such that one or two synoptic (or convective) events can bring about the end of a meteorological drought. Thus, the purpose of this study is to analyze the synoptic-scale meteorology of the assigned 1999–2005 drought. In the context of this drought being different compared to historical Canadian Prairie droughts, the aim of this study is to diagnose the quasi-geostrophic (QG) mechanisms for subsidence and unique synoptic-scale forcings/conditions that lead to the dry conditions during this study period. Key severe periods during the drought are identified and then analyzed synoptically by examining dynamic and thermodynamic fields.

1.4 Structure/Outline

The structure of the remaining chapters will proceed in the following order. Chapter 2 discusses the data used in this drought study. Chapter 3 deals with the methods used in the diagnosis of key periods and analysis of the drought, and addresses issues that emerged from the reanalysis data. Chapter 4 discusses the results, and a summary and conclusions will constitute Chapter 5.

CHAPTER 2

Data

2.1 Precipitation Data

2.1.1 Precipitation Station Data

Corrected precipitation data at a monthly timescale were obtained from Environment Canada's Climate Research Division Adjusted and Homogenized Canadian Climate Data (AHCCD), freely available on the web (http://www.cccma.bc.ec.gc.ca/hccd/index_e.shtml). Corrected daily precipitation data for Alberta, Saskatchewan, and Manitoba have also been provided by the Climate Research Division through Éva Mekis. These data have been corrected for known inhomogeneities and systematic biases, which include gauge errors arising from wind, evaporation, and wetting losses, but also errors from changes in instrumentation, measurement procedures, the location of stations (Mekis and Hogg 1999). The issues of trace amounts and missing data were also dealt with in the procedure. These data were obtained in order to provide a historical perspective of Canadian Prairies drought and to identify key severe periods in 1999–2005.

2.1.2 Global Precipitation Climatology Project, GPCP

To view the spatial representation of precipitation deficits during the drought, the GPCP Version 2.1 combined satellite-station precipitation dataset (Alder et al. 2003) was obtained from National Oceanic & Atmospheric Administration / Office of Oceanic and Atmospheric Research / Earth System Research Laboratory Physical Sciences Division (NOAA/OAR/ESRL PSD), freely available on the web at http://www.esrl.noaa.gov/psd/data/gridded/data.gpcp.html. This dataset is comprised of monthly mean precipitation rates from January 1979–September 2009 at a 2.5° by 2.5° resolution. GPCP V.2.1 combines low-orbit microwave and geosynchronous-orbit infrared satellite data with surface rain gauge observations, and is part of the World Climate Research Program (WCRP) Global Energy and Water Cycle Experiment (GEWEX) (Alder et al. 2003).

2.2 Dai PDSI dataset

For additional spatial representation of the drought, the Dai PDSI dataset (Dai et al. 2004) was obtained from NOAA/OAR/ESRL PSD, freely available on the web at http://www.esrl.noaa.gov/psd/data/gridded/data.pdsi.html. This dataset includes monthly PDSI values, ranging from approximately -10 (drought) to $+10$ (wet), at a 2.5° by 2.5° resolution.

2.3 Teleconnection Index (PNA)

For the purposes of a planetary-scale outlook, daily PNA indices were obtained from NOAA National Weather Service / National Centers for Environmental Prediction / Climate Prediction Center (NWS/NCEP/CPC), freely available on the web at http://www.cpc.noaa.gov/products/precip/CWlink/daily_ao_index/history/history.shtml.

2.4 Atmospheric Soundings

To provide additional vertical detail in the synoptic-scale analysis, atmospheric soundings for Edmonton Stony Plain (CWSE) were obtained from the University of Wyoming website (http://weather.uwyo.edu/upperair/sounding.html).

2.5 Reanalyses

2.5.1 NCEP/NCAR Global Reanalysis

The meteorological fields will be displayed using the Global National Center of Environmental Prediction / National Center for Atmospheric Research (NCEP/NCAR) Global Reanalysis (Kalnay et al. 1996), which has a spatial resolution of 2.5° by 2.5°. The temporal resolution is 4 times daily (every 6 hr), and is available from 1948 to present.

2.5.2 North American Regional Reanalysis, NARR

The NARR (Mesinger et al. 2006) was also used, as it provides data at a much finer temporal (8 times daily, every 3 hr) and spatial (32 km) resolution from 1979–present. Theoretically, this reanalysis should be superior to the NCEP/NCAR Global Reanalysis because of the finer resolutions. However, for the reasons outlined in Section 3.2.1, the NCEP/NCAR Global Reanalysis was chosen for the display of meteorological fields in Chapter 4.

Reanalysis variables were calculated and displayed using Grid Analysis and Display System (GrADS) Version 2.0.a8, supplied by the Center for Ocean-Land-Atmosphere Studies (COLA) (Doty 1988).

CHAPTER 3

Methods

3.1 Brief Historical Perspective

Monthly precipitation accumulation values were averaged over 33 stations in the Prairies (Fig. 3.1) to create one homogeneous monthly time series from 1948–2005. These stations were chosen on the basis of record length (1948–2005), even spatial coverage representative of the study region, relatively few missing data, and having both monthly and daily corrected precipitation data. This monthly time series is representative of an areal average over the Prairies. A 30-year monthly climatology for the 33-stations for the period 1976–2005 was also computed using the monthly corrected data. The 30 years from 1976–2005 were used for the climatology as opposed to another period (e.g. 1971–2000) so that it would be inclusive of the drought years. From this, monthly anomalies were then computed by subtracting the monthly climatological value from the corresponding value in the time series. This provides a brief historical perspective of drought in the Prairies.

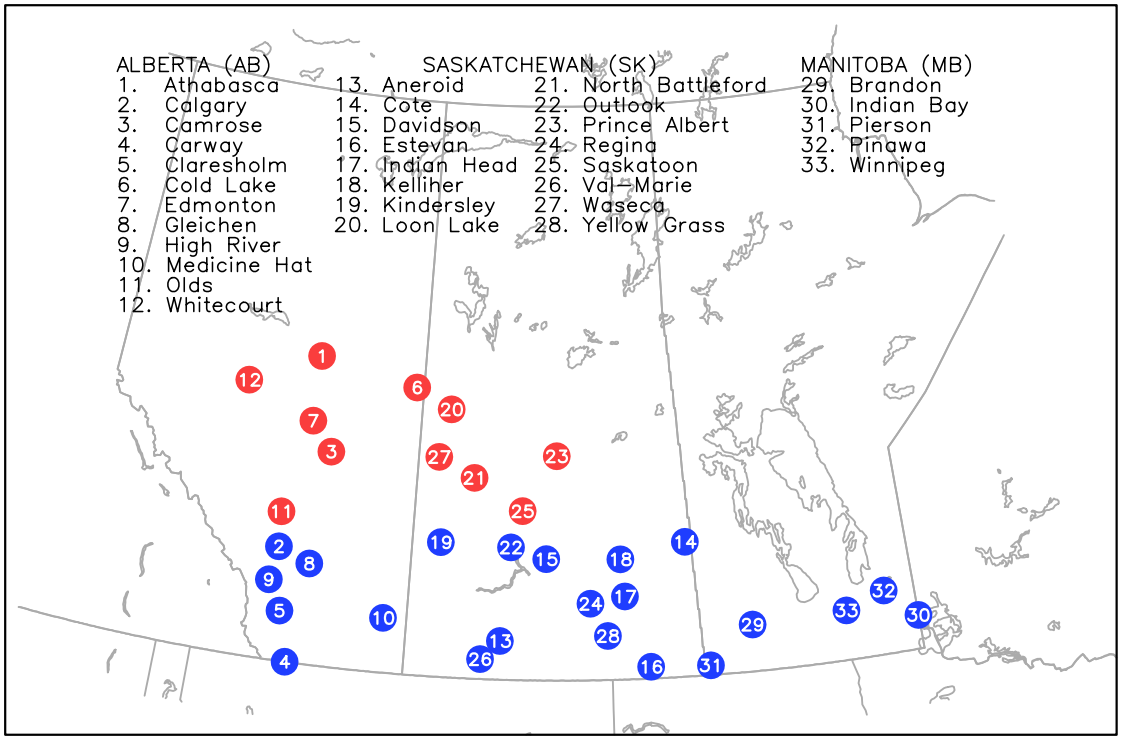

Figure 3.1: The domain includes the 33 stations plotted and listed above. The red stations delineate a northern partitioning of the stations, and blue stations are southern stations.

3.2 Diagnosis/Identification of key periods

A few methods were explored in order to identify key "case study" periods – the driest, or most severe, meteorologically speaking – during the 1999–2005 drought in which to study using QG theory on a synoptic temporal and spatial scale. Since one or two synoptic events can effectively end a meteorological drought, temporal resolution smaller than a month or season needed to be scrutinized. Drought indices such as the PDSI and SPI were deemed ineffective for looking at timescales less than a month.

3.2.1 Moisture Divergence

One possible avenue that was explored for the purpose of diagnosing the key severe periods was through vertically integrated moisture divergence. Initially, the

concept of using moisture divergence as an identifier seemed ideal, because in a basic sense, moisture divergence is essentially $Evaporation - Precipitation$. Positive values indicates that evaporation is greater than precipitation, giving rise to a moisture balance deficit, and thus theoretically an indicator of meteorological drought conditions. However, this computed quantity did not provide the expected detail, and it produced some surprising results in terms of the use and integrity of the reanalysis data.

The total balance equation for water vapour in the atmosphere is as follows (Peixoto and Oort 1992):

$$\frac{\partial W}{\partial t} + \nabla \cdot \mathbf{Q} + \frac{\partial W_c}{\partial t} + \nabla \cdot \mathbf{Q_c} + P = E \tag{3.1}$$

where

W is the amount of precipitable water, $W = \frac{1}{g}\int_0^{p_0} q \, \mathrm{d}p$, (i.e. specific humidity, q, integrated from the earth's surface, p_0, to the top of the atmosphere)

$\mathbf{Q}$ is the horizontal transport vector of water vapour, $\mathbf{Q} = \frac{1}{g}\int_0^{p_0} \mathbf{v} q \, \mathrm{d}p$

W_c is the amount of condensed water in a unit column, $W_c = \frac{1}{g}\int_0^{p_0} q_c \, \mathrm{d}p$

$\mathbf{Q_c}$ is the horizontal transport vector of condensed water, $\mathbf{Q_c} = \frac{1}{g}\int_0^{p_0} \mathbf{v} q_c \, \mathrm{d}p$

P is Precipitation, and

E is Evaporation.

But since

$$\frac{\partial W_c}{\partial t} \ll \frac{\partial W}{\partial t} \quad \text{and} \quad \mathbf{Q_c} \ll \mathbf{Q}, \tag{3.2}$$

then Equation (3.1) becomes (after time averaging),

$$\overline{\frac{\partial W}{\partial t}} + \nabla \cdot \overline{\mathbf{Q}} + = \overline{E} - \overline{P} \tag{3.3}$$

where the bar operator indicates time averaging. Over a long enough time, the storage term, $\frac{\partial W}{\partial t}$ can also be neglected, to give:

$$\nabla \cdot \overline{\mathbf{Q}} = \overline{E} - \overline{P} \tag{3.4}$$

Thus, moisture divergence was calculated first using the NARR fields for surface pressure, mixing ratio, and wind for each 3 hr time interval from 1979–2008 using Equation (3.4), with the upper limit of the integration adjusted to 150 hPa. The 3-h values were then averaged over each month, and a monthly climatology was then created from these values for the 30-year period from 1979 to 2008. Monthly anomalies were then computed by subtracting the value for each month in the time series by the corresponding climatological value. Figures 3.2a and 3.2b show respectively a time series of areal averaged anomalous and total moisture divergence for a $5^\circ \times 10^\circ$ box in the Palliser Triangle region (49°–54°N, 103°–113°W). As outlined in Milrad et. al (2010, personal communication), there is an abrupt reversal in the sign of the moisture divergence anomaly in 2002, from largely more divergent than normal to more convergent than normal after 2002. A similar change occurs in the total field, but is less dramatic than the anomaly. For comparison, moisture divergence was also computed using the NCEP/NCAR Global Reanalysis in the same method using Equation (3.4) (however, only to 300 hPa, owing to moisture data availibility). It is clear from the monthly anomaly plot for the same area for the Global Reanalysis (Fig. 3.2c) that this abrupt change does not occur in 2002. The monthly NARR anomaly plot for an area just south of the Canadian box (44°–49°N, 103°–113°W), is also shown in Fig. 3.2d. Unlike the time series for the area in Canada, there is no dramatic change in 2002. Thus, as suggested by Milrad et. al (2010, personal communication) this abrupt reversal of sign in the NARR moisture divergence for the area in Canada can be attributed to the precipitation assimilation change that occurred in 2002 in the NARR for Canada. In 2002, the precipitation assimilation in Canada changed from gauge-only data to model-only data. It is known that there are problems with NARR precipitation in Canada (Milrad et al. 2009; Mesinger et al. 2006; Karnauskas et al. 2008). However, it was unprecedented that this assimilation change would show up in the mass fields, as seen through moisture divergence. Because this assimilation change occurred in the middle of the 1999–2005 period, and the possible effect on the mass fields, the decision was made to use the NCEP/NCAR Global Reanalysis for the synoptic analysis as op-

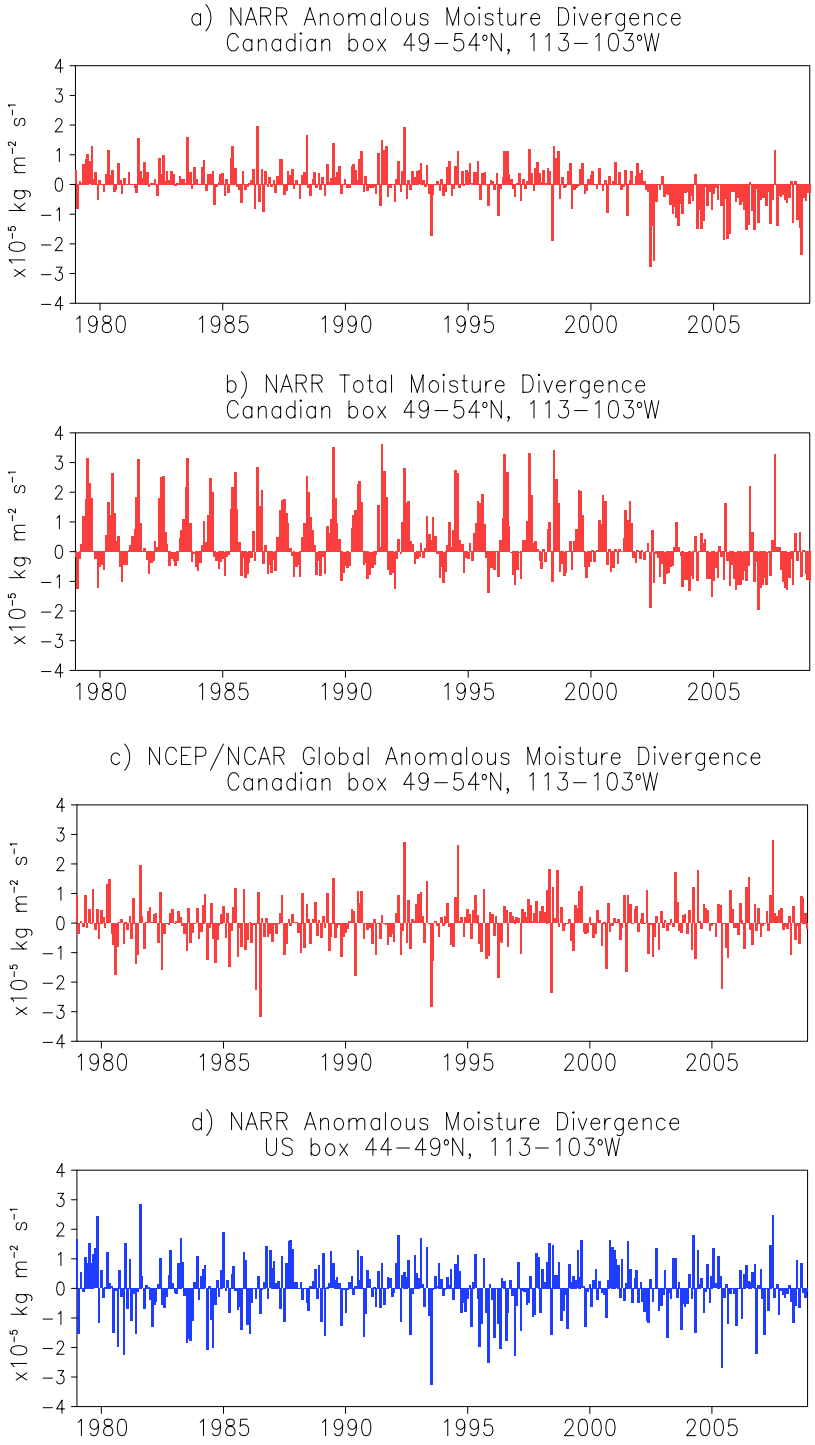

Figure 3.2: a) NARR Anomalous and b) Total Moisture divergence for Canadian box. c) NCEP/NCAR Global Anomalous moisture divergence. d) NARR Anomalous moisture divergence for US box.

posed to the NARR. Again, this technique was discarded as a method of diagnosing the key dry periods because it did not show extended periods of anomalous moisture divergence as would be expected during a drought period. As shown in Fig. 3.2c, the 1999–2005 interval cannot be easily distinguished from the remaining periods of the time series as grossly more divergent than normal. Thus, another technique needed to be considered in order to identify our key dry periods.

3.2.2 Precipitation: Daily Percent of Climatology

The method established for identifying key severe periods in this study uses daily and monthly precipitation station data in a modified daily percentage of climatology technique. Daily precipitation values were averaged over 33 stations (Fig. 3.1) from 1999–2005. The 30-year monthly climatology (averaged for the 33-stations) for the period 1976–2005, as mentioned above in Section 3.1, is also used in this procedure. The terms "percent of normal" and "percent of climatology" refer to the same idea, and will be used interchangeably. In addition, the spatially variant argument against the percent of normal concept does not hold here as the stations are close enough together to be considered occupying the same location.

The first step in this percentage of normal technique involves deriving a daily climatology of precipitation accumulation from a monthly climatology. The process is as follows:

1. The monthly value of accumulated precipitation (in mm) is divided by the number of days in the respective month (i.e. January 31 days, February 28.25 days, etc.) to get a "daily" value. For example, if the climatology for May is 60 mm, the "daily" value would be 60 mm/31 days = 1.935 mm day^{-1}

2. Instead of assigning this one value to every day in the month, giving a "blocky" climatology, this "daily" value is assigned only to the middle (15th day) of the month. Following the previous example, the value of 1.935 mm day^{-1} is assigned to 15 May.

3. Linear interpolation is then carried out from mid-month to mid-month to

achieve values for all of the other days in the year, to show the increase or decrease in accumulation between months. The values for the remaining days in each month are thus determined by the climatology of 2 months. For example, the values for the beginning half of May are dependent on April and May climatology, whereas the values after 15 May are a combination of both May and June climatology.

The end result from this process is a finer temporal scale climatology (daily, 365 values) interpolated/created from a monthly climatology (12 values). This was needed in order to compute the percentage of normal on a daily basis. The percentage of normal quantity was derived by dividing the actual accumulation value for each day in the time series, P_i by the "expected" value for that day from the daily climatology, P_{ci},

$$\text{Percentage of Normal}_i = \frac{P_i}{P_{ci}} \tag{3.5}$$

This procedure gives a percentage of climatology for each day in the time series (1999–2005). These values are then smoothed by taking 30-day running averages, or 30-day moving windows, with the averaged value assigned to the middle of the period. For example, the average for 1 to 30 May 1999 is assigned to 15 May 1999, and the average for 2 to 31 May 1999 is assigned to 16 May 1999, etc. The reason for calculating this indicator for meteorological drought on a daily basis, and then computing 30-day running means proceeds from the fact that completing a synoptic study of a drought engages two timescales – the synoptic timescale (two–three days) and the much longer timescale of drought (one month to five+ years). This methodology attempts to provide a longer time filter while keeping the daily/synoptic timescale memory, thus amalgamating the long duration timescale of drought with the synoptic timescale. Another advantage of using 30-day running means is that this does not limit the view of the drought to the bounds of a month – this allows for 30-day periods, and thus maximum and minimum values, to occur mid-month to mid-month.

Finally, the lowest ten points of the 30-day running mean time series are identified as the ten driest 30-day periods, and the five highest peaks as the five wettest

30-day periods for comparison.

3.3 Meteorological Analysis of key periods

The primary goal in the synoptic-scale analysis of the identified key dry periods is to examine the mechanisms that inhibit precipitation formation, namely descent or subsidence. Vertical motion in the atmosphere is represented by the adiabatic, frictionless form of the QG omega equation, as outlined in Bluestein (1992):

$$\left(\nabla_p^2 + \frac{f_0^2}{\sigma}\frac{\partial^2}{\partial p^2}\right)\omega = -\frac{f_0}{\sigma}\frac{\partial}{\partial p}\left[-\mathbf{v_g}\cdot\nabla_\mathbf{p}(\zeta_g + f)\right] - \frac{R}{\sigma p}\nabla_p^2(-\mathbf{v_g}\cdot\nabla_\mathbf{p}T) \tag{3.6}$$

where

f_0 is the constant Coriolis parameter (s^{-1})

σ is the static stability parameter, $\frac{-RT}{p}\frac{\partial ln\theta}{\partial p}$ ($m^2\ s^{-2}\ Pa^{-2}$)

θ is potential temperature (K)

ω is the vertical velocity ($Pa\ s^{-1}$)

ζ_g is the relative vorticity of the geostrophic wind (s^{-1})

f is the latitude-dependent Coriolis parameter (s^{-1})

p is pressure

R is the universal gas constant ($287\ J\ kg^{-1}\ K^{-1}$)

$\mathbf{v_g}$ is the geostrophic wind vector ($m\ s^{-1}$), and

T is temperature (K)

The first term of the right-hand side (RHS) of Equation (3.6) is the change of geostrophic vorticity advection with respect to pressure. This term represents the forcing for descent ($\omega > 0$) for regions of upper-level anticyclonic vorticity advection (AVA, e.g. downstream of a vorticity minima in a ridge axis) $-\mathbf{v_g}\cdot\nabla_\mathbf{p}(\zeta_g + f) <$

0, with the assumption that vorticity advection at the surface is negligible (i.e. decreasing vorticity advection with height). By continuity (Bluestein 1992),

$$-\frac{\partial \omega}{\partial p} = \nabla_{\mathbf{p}} \cdot \mathbf{v} = \delta \tag{3.7}$$

descent is associated with surface divergence in level terrain, and thus the formation of a surface high pressure system. This is the mechanism involved in the traditional ridging paradigm of drought in the Canadian Prairies (see Section 1.2.3).

The second term on the RHS of Equation (3.6) is the horizontal Laplacian of geostrophic temperature advection. This term represents the forcing for descent ($\omega > 0$) for a local maximum of cold air advection (CAA), $-\mathbf{v_g} \cdot \nabla_{\mathbf{p}} T < 0$. Thus, CAA is another synoptic-scale mechanism associated with descent, and thus dry conditions.

Descent, or subsidence, can also be caused orographically as westerly trajectories are forced up and over the Rocky Mountain Range (i.e. when the wind is perpendicular to terrain) and descend on the lee side into the Prairies. This is known as downslope flow. Moisture is precipitated out on the windward side and air parcels descend and warm adiabatically on the lee side, causing the aforementioned rainshadow effect in the Prairies. Considering only orographically induced vertical motions, and in the absence of the above dynamical forcing, the homogeneous QG omega equation can be expressed at the surface as (Bluestein 1993):

$$\nabla_p^2 \omega_0 = -\frac{f_0^2}{\sigma} \frac{\partial^2 \omega_0}{\partial p^2} \tag{3.8}$$

Downslope motion, $\omega > 0$, under positive static stability makes for

$$\frac{\partial^2 \omega_0}{\partial p^2} > 0 \tag{3.9}$$

This combined with continuity (3.7), leads to convergence increasing with decreasing height:

$$-\frac{\partial \delta}{\partial p} > 0 \tag{3.10}$$

and thus convergence and increasing cyclonic vorticity at the surface. Consequently, flow over terrain results in high pressure on the windward side, associated

with upslope flow, and conversely a low pressure on the leeward side, associated with downslope flow. This is the surface signature of a downsloping event. The lee of the mountains is in fact a region of cyclogenesis (Bluestein 1993). However, the adiabatic warming and drying associated with the orographic descent often overwhelms the development of precipitation if there is no advection of moisture into the area. Thus, since the Rocky Mountain Range acts as a barrier to moisture from the Pacific, moisture must be advected from the Gulf of Mexico in order to get sufficient moisture on the lee side of the Rockies for large precipitation events in the Prairies.

Therefore, in order to analyze the QG forcings for the drought, synoptic scale upper- and lower-level fields are averaged for the identified 30-day periods. Here, mechanisms in the identified dry periods are compared and contrasted with those for the wet periods. Wind and geopotential height at the 300-hPa level are examined to determine upper-level structure and vorticity advections. MSLP and 1000–500-hPa thickness and thickness anomalies are also examined for storm tracks, temperature advections, and temperature anomalies. Since moisture availability is also important for the production, or absence, of precipitation, precipitable water anomalies and low level (1000–700 hPa) moisture transport are examined at the 700-hPa level. It should be noted that 30-day mean fields have a potential of smearing, particularly if there is great variability about the pattern during the 30-day period. In order to solve this issue, and to give a finer temporal resolution of the synoptic-scale forcings, time-height vertical cross sections of temperature and vorticity advections, relative and specific humidity, and omega, and are also examined. The daily PNA values and atmospheric soundings also help to eradicate the smearing in the 30-day mean fields.

CHAPTER 4

Results and Discussion

4.1 Overview of the drought

4.1.1 Temporal Representation

To provide a brief historical perspective of Canadian Prairie drought, 33-station monthly mean precipitation anomalies (Fig. 4.1) and percentages of climatology (Fig. 4.2) are presented in Hovmöller-like diagrams (Hovmöller 1949) from 1948 to 2005. The 33-station mean is representative of an areal average over the study area (see Fig. 3.1). Similar structures are seen in both figures, with below-normal features in 1960s, 1980s, and 2000s, corresponding to drought periods, and relatively wet periods in 1953–54 and in the 1990s. As expected, the largest precipitation anomalies (Fig. 4.1) occur primarily during the growing season months (here defined as April through September) when, climatologically, most of the precipitation occurs. Anomalies in the growing season can have a greater magnitude than the total accumulation in the cool season, thus masking out cool season anomalies. In particular, June and August 1961, July 1985, and August 2001 stand out in Fig. 4.1 (marked A, B, C, and D, respectively) as being the four months in the entire period with departures of more than 40 mm. The 1988 drought, which had

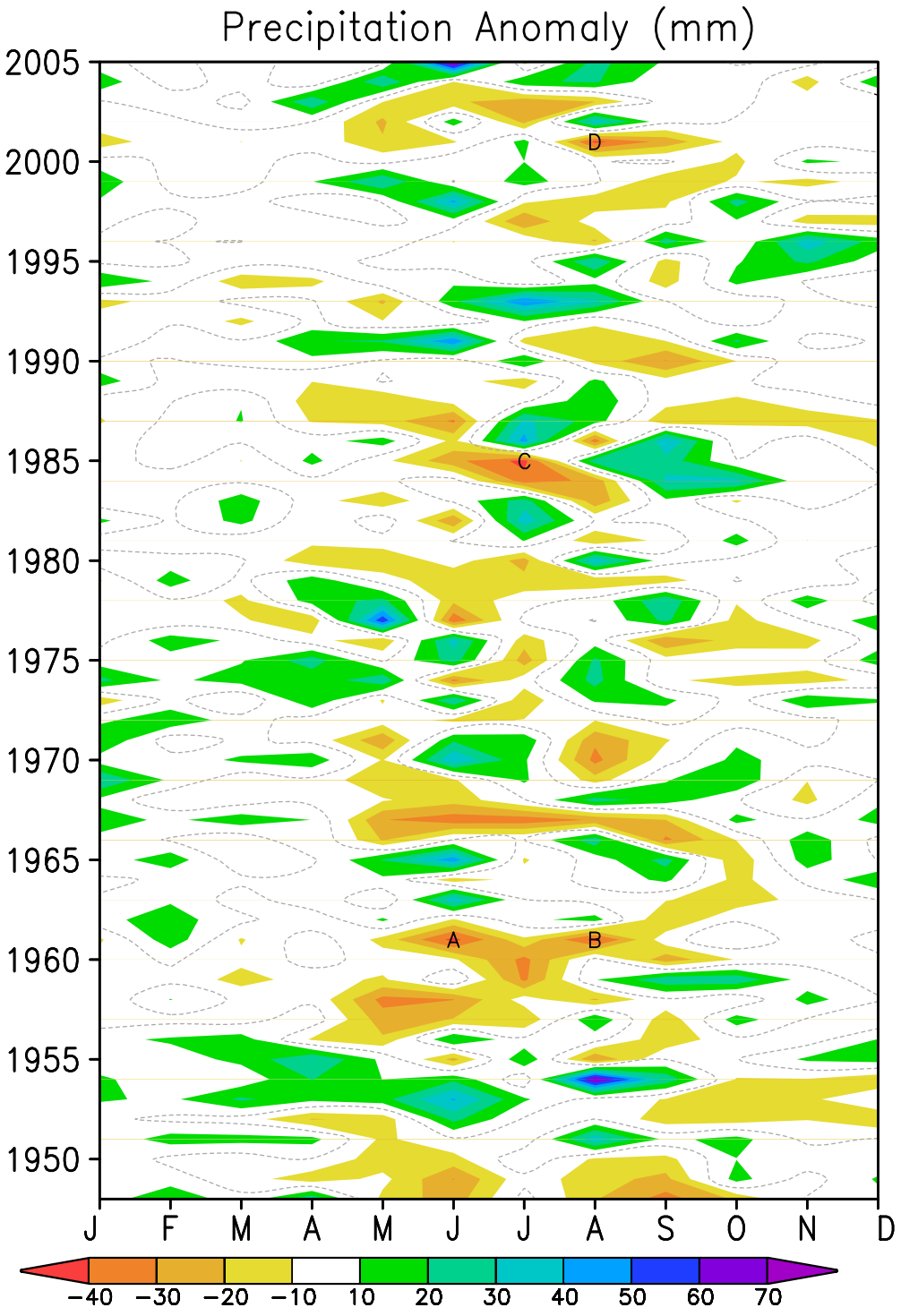

Figure 4.1: Precipitation anomaly (mm), averaged over the Palliser Triangle region (33 stations), for 1948–2005, relative to 1976–2005 climatology. The notations A, B, C, and D refer to particularly severe dry dates as referred to in the text.

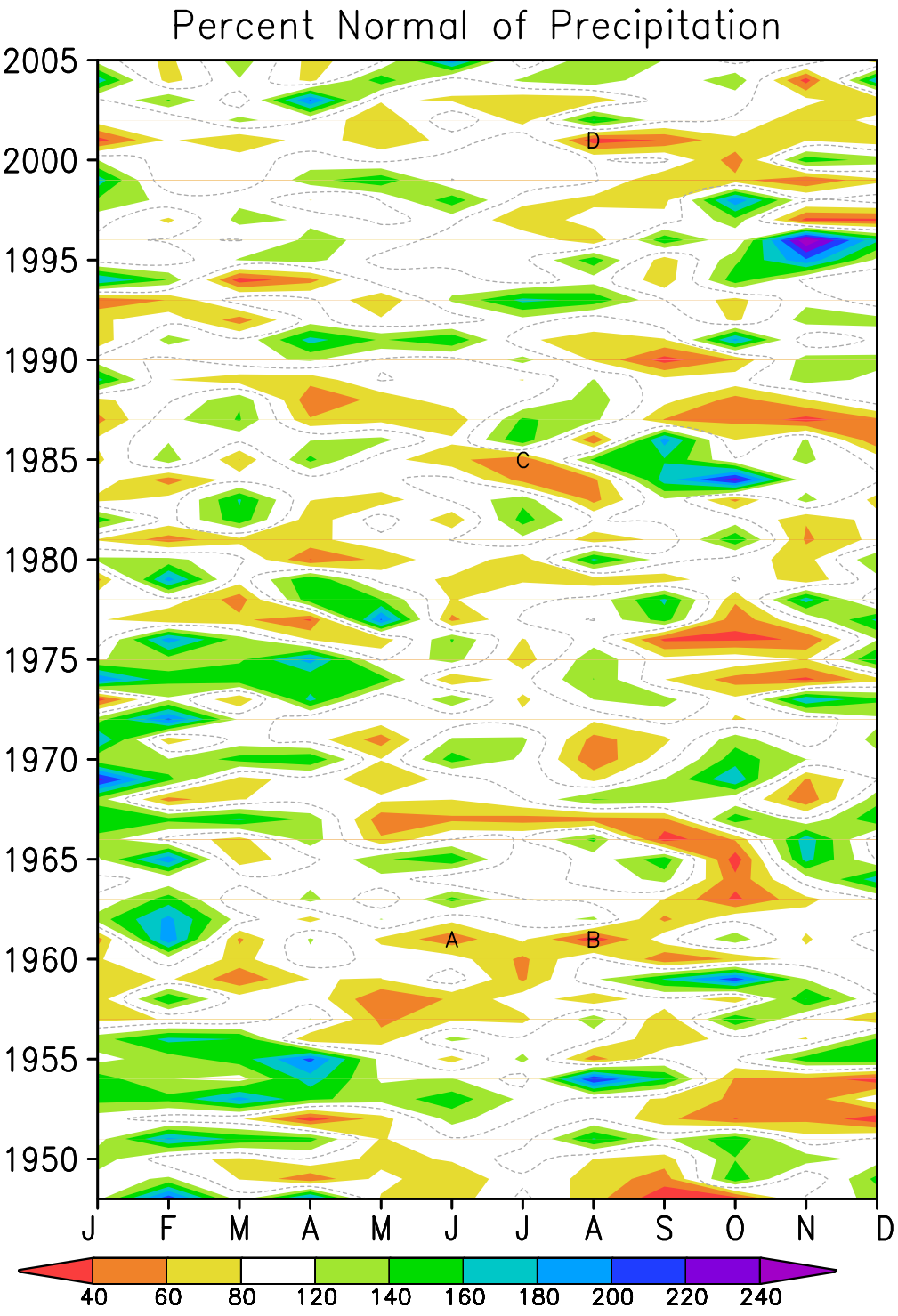

Figure 4.2: Percent of climatology for precipitation, averaged over the Palliser Triangle region (33 stations), for 1948–2005, relative to 1976–2005 climatology. The notations A, B, C, and D refer to particularly severe dry dates as referred to in the text.

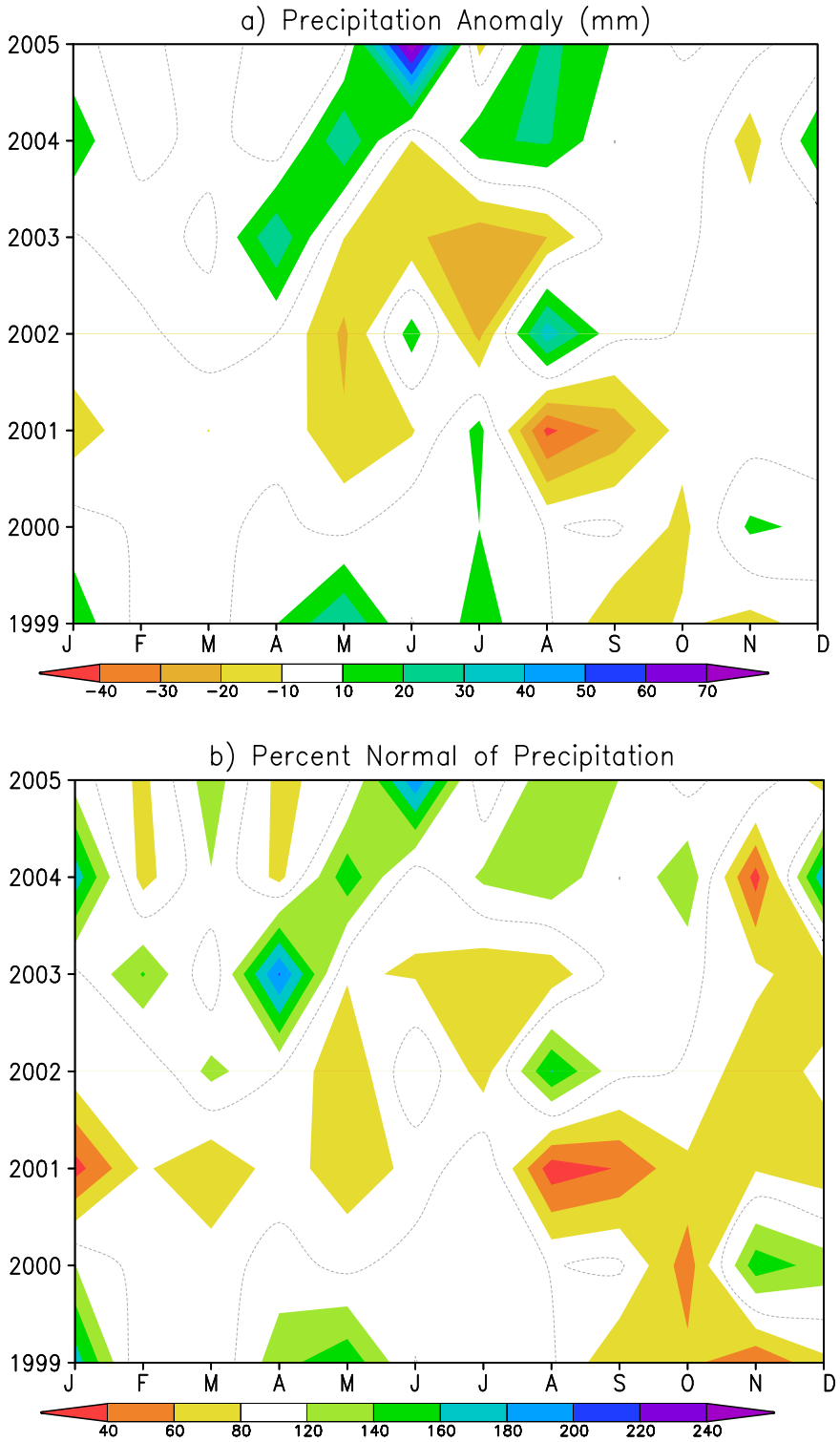

Figure 4.3: a) As in Fig. 4.1, but for the 1999-2005 drought period. b) As in Fig. 4.2, but for the 1999-2005 drought period.

significant agricultural impacts, does not manifest itself as a significant departure from normal, as this drought mainly had to do with the timing of precipitation. As mentioned above and in Wheaton et al. (2008), precipitation came too late for crop growth in 1988. The percentage of climatology (Fig. 4.2) highlights the importance of dry autumn seasons, especially in 1963–65 and in 1998–2000. The above normal values in January-February-March (JFM) of 1948–1976 in Fig. 4.2 may be the result of what appears to be an overall drying of these months in the discretized period of 1976–2005, from which the climatology was computed. Surprisingly, however, it is rather difficult to single out the entire 1999–2005 period as compared to the rest of the time series in both Figs. 4.1 and 4.2; at best, only 2001–2002 are notable.

Figures 4.3a and 4.3b give a closer look of the specific 1999-2005 period. Again, similar structures are seen in both figures, with the cool season given more emphasis in the percent of climatology (Fig. 4.3b). The most significant departures from normal begin in autumn of 1999. Departures from climatology wane in the growing season of 2000, but return in autumn of 2000. All months of 2001 (except July) are below normal, especially August 2001 which reaches a negative anomaly below -40 mm, and is also less than 40% of normal. The dry months in 2002 of May and July are interspersed in between slightly wet months of June and August. In 2003, the beginning of the growing season (April) is rather wet, which initiates the recovery from drought, but dry conditions return in the following summer months. 2004 and 2005 are for the most part wetter than normal, with the exception of November 2004.

We conclude, upon examining Fig. 4.3, that the 1999–2005 drought peaked in severity during in 2001 and 2002, with the significant precipitation deficits beginning in the autumn of 1999, and ending in 2004. Furthermore, Figs. 4.1 and 4.2 show that the 1999–2005 period was not a particularly exceptional meteorological drought, as compared with other dry periods during 1948–2005. The same conclusion has been articulated in other studies (e.g. Bonsal and Regier 2007).

4.1.2 Spatial Representation

As noted by Bonsal and Wheaton (2005), the spatial pattern of the 1999–2005 drought was unique in terms of its northward extent, particularly in 2001 and 2002. Figure 4.4 is the average PDSI, from the Dai PDSI dataset, (Dai et al. 2004), for the entire 1999–2005 period. The PDSI field is primarily negative in the study area, yet the drought appears especially prominent in the north, where PDSI values below -10 are seen. However, the horizontal structure of the 1999–2005 drought, as with any drought, did vary from season to season (not shown).

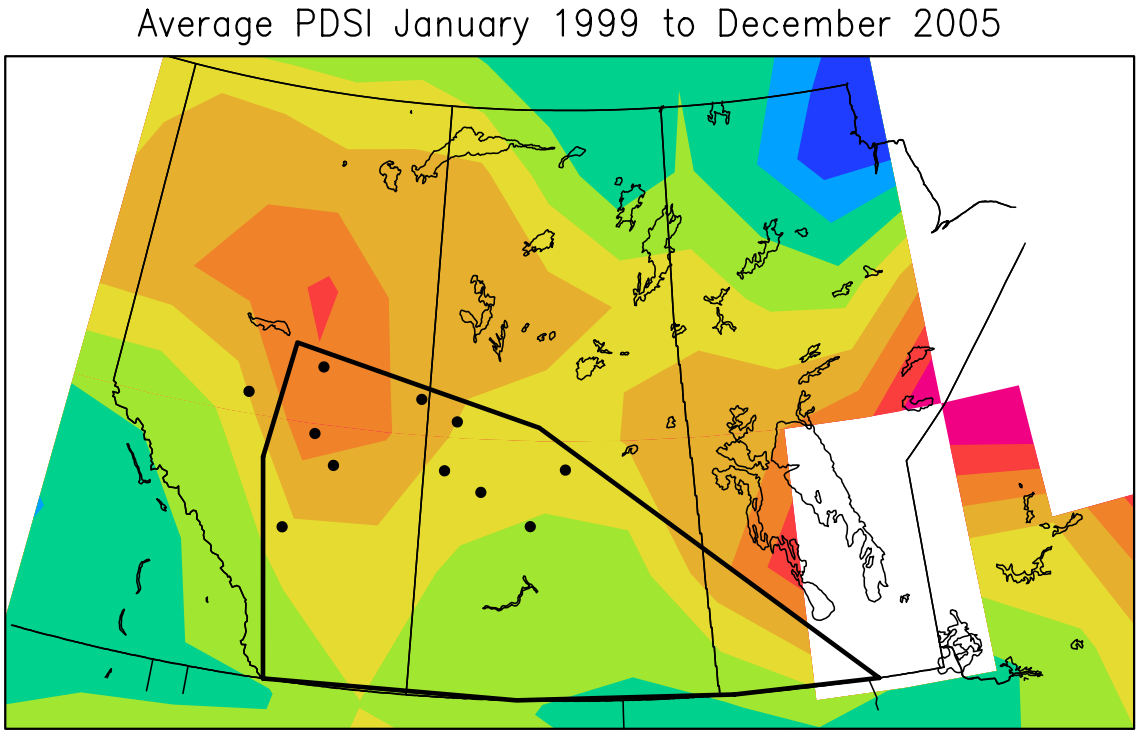

Figure 4.4: Averaged PDSI for 1999–2005 over the Prairies. The northern stations are plotted, as is the approximate outline of the study region. Note that the gap in southern Manitoba is due to missing data.

The spatial pattern of GPCP percent normal precipitation during the 2001–2002 growing season months of April through September is also variable (Fig. 4.5). The spatial extent of the drought is greatest in 2001, with values of less than 80% of normal covering most of the southern halves of both Alberta and Saskatchewan, the epicentre of which is located on the border of the two provinces. Areas below

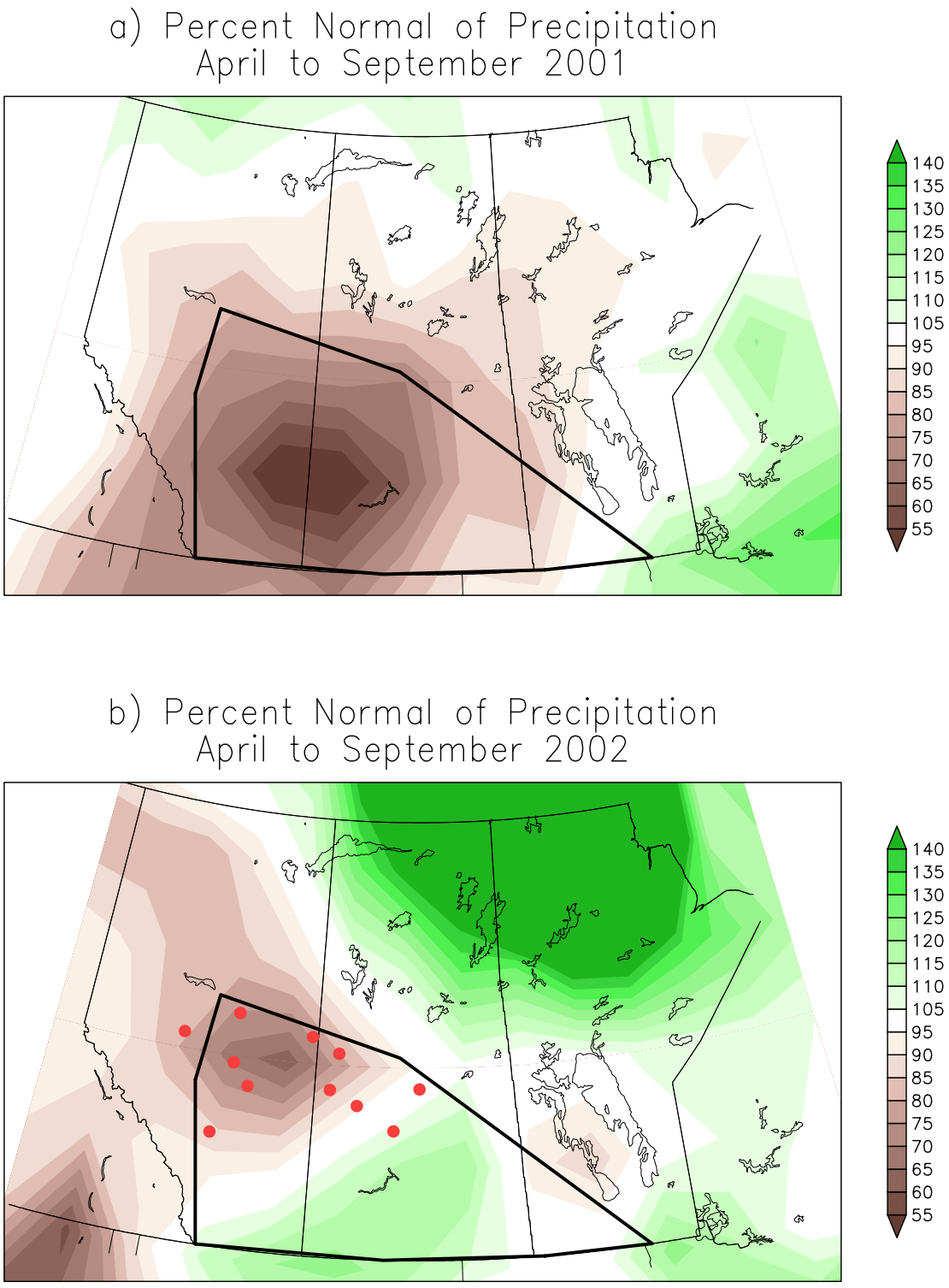

Figure 4.5: Percent Normal of GPCP Precipitation, for the growing seasons of a) 2001 and b) 2002. The outline is the approximate extent of the study area.

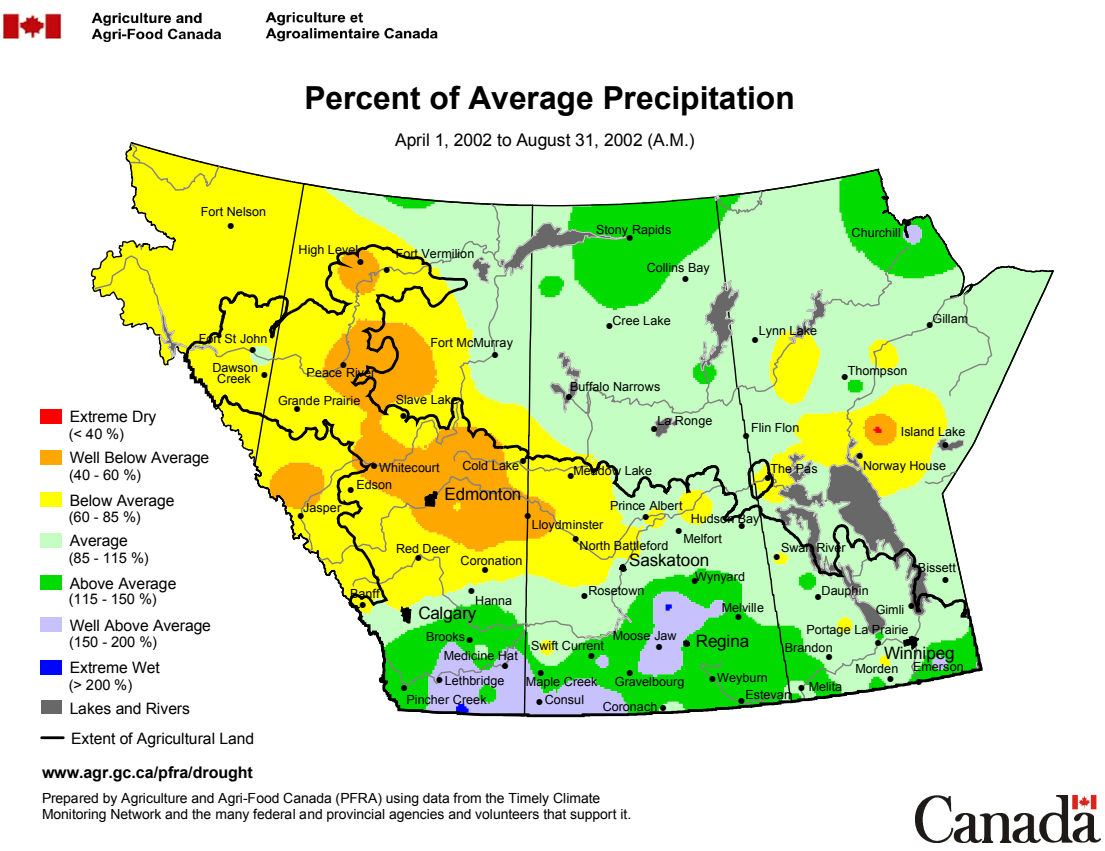

Figure 4.6: Percent Normal for the Growing Season of 2002 from Agriculture and Agri-Food Canada (cited 2010).

normal extend east to Manitoba and close to the northern borders of the Prairie provinces (Fig. 4.5a). This pattern differs from the 2002 growing season (Fig. 4.5b), which is marked by a shift of the focal drought point northeastward to the eastern border of Alberta. A feature that is worthy of more attention in Fig. 4.5b is the region of above-normal precipitation in southern Saskatchewan. This is highly interesting and highlights the complexity of this drought. A meteorological drought does not entail a complete absence of high precipitation events, but rather a decrease in the number of such events (Evans 2008). Closer inspection reveals that there were a few large precipitating events in the southern parts of the Prairie provinces in June 2002 (not shown). This proximity of above- and below- normal precipitation emphasizes the extreme spatial variability of precipitation in the Prairies. The precipitation analysis from Agriculture and Agri-Food Canada (Fig.

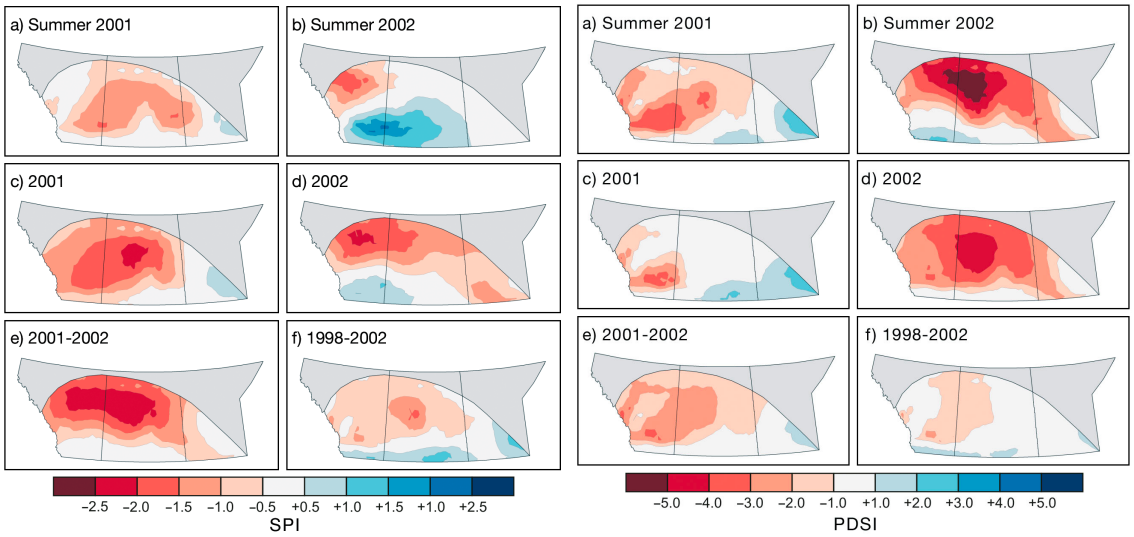

a b

Figure 4.7: a) SPI and b) PDSI for the drought period. Taken from Figs. 2 and 3 from Bonsal and Regier (2007).

4.6) and the SPI and PDSI analysis of Bonsal and Regier (2007) (see Figs. 4.7a and 4.7b) also show this high-low couplet of above- and below- normal precipitation in the growing season of 2002. It is particularly apparent in the SPI and PDSI for Summer 2002, as well as in SPI for 2001–2002 Fig. 4.7.

The presence of this "wet" feature in the study region could present an issue when completing the identification technique outlined in Section 3.2.2, i.e. the 33-station "areal" averages of the daily percent of climatology. To avoid masking the drought signature and thus failing to capture some key periods, a northern subset of the 11 stations from the original 33 was chosen to complete the diagnosis of key severe 30-day periods in the next section. This northern subset is seen in Figs. 4.4 and 4.5, as well as the red stations in Fig. 3.1 with its southern boundary at approximately 51.75°N.

4.2 Identification of key periods

The results of the identification process (i.e. 30-day running mean filter on the daily percent of climatology from January 1999 to December 2005, Section 3.2.2) for the

northern subset of stations, shown in Fig. 4.8a, are compared with the time series of the same diagnostics for Saskatoon (CYXE, #25 in Fig. 3.1) in Fig. 4.8b and for the 33-station mean in Fig. 4.8c. There is a general decreasing trend from the beginning of 1999 to autumn of the same year for the northern stations in Fig. 4.8a, during which time values fall to below 30%. A slight reprieve from meteorological drought conditions occurs in early to mid- 2000 in Fig. 4.8a, but abruptly drops to below 30% in autumn of 2000 and continues to oscillate below 150% with no extended recovery until 2003. The precipitation peaks from autumn 2000 to the end of 2002 are not as frequent or as high-yielding as they are on the flanking years (i.e. 1999 and 2003–2005), indicating a reduction of large precipitation events during the heart of the drought. The key severe dry and wet periods that will be examined synoptically in the next section are identified in Fig. 4.8a as the lowest ten (in red) and the top five (in green) 30-day running mean values for the northern stations in the 1999–2005 period. These identified events are listed with their central date in descending severity in Tables 4.1a and 4.2a. As expected, the frequency of the identified dry events is the greatest during the heart of the drought from autumn of 2000 to 2002, and the top five values occur on the flanking years (1999, 2003–2005). It is also of note that the identified dry events in Table 4.1a are slightly skewed to autumn and winter periods, owing to the climatological paucity of precipitation in these seasons.

Table 4.1: Dry Events: Lowest 10 values of a) northern stations time series (Fig. 4.8a) and b) 33-station time series (Fig. 4.8c). The northern station dates are denoted in red in Fig. 4.8a. The * indicates an identified key period that is unique to the northern stations.

(a) Northern Stations

Central Date	30-day percentage
1) 29 December 2001	12.72%
2) 30 November 2002	18.35%
3) 18 October 2000	19.51%
4) 20 May 2002*	21.23%
5) 21 January 2001	21.68%
6) 28 April 2001	21.81%
7) 12 December 2003	22.99%
8) 8 November 2004	23.05%
9) 15 October 1999*	24.12%
10) 30 April 2005	28.09%

(b) 33 Stations

Central Date	30-day percentage
1) 7 October 2000	18.41%
2) 20 August 2001	19.55%
3) 10 December 2003	29.17%
4) 16 January 2001	19.42%
5) 14 November 2004	19.85%
6) 1 December 2002	30.79%
7) 7 October 2003	32.20%
8) 29 April 2001	32.41%
9) 30 April 2005	35.24%
10) 27 December 2001	35.22%

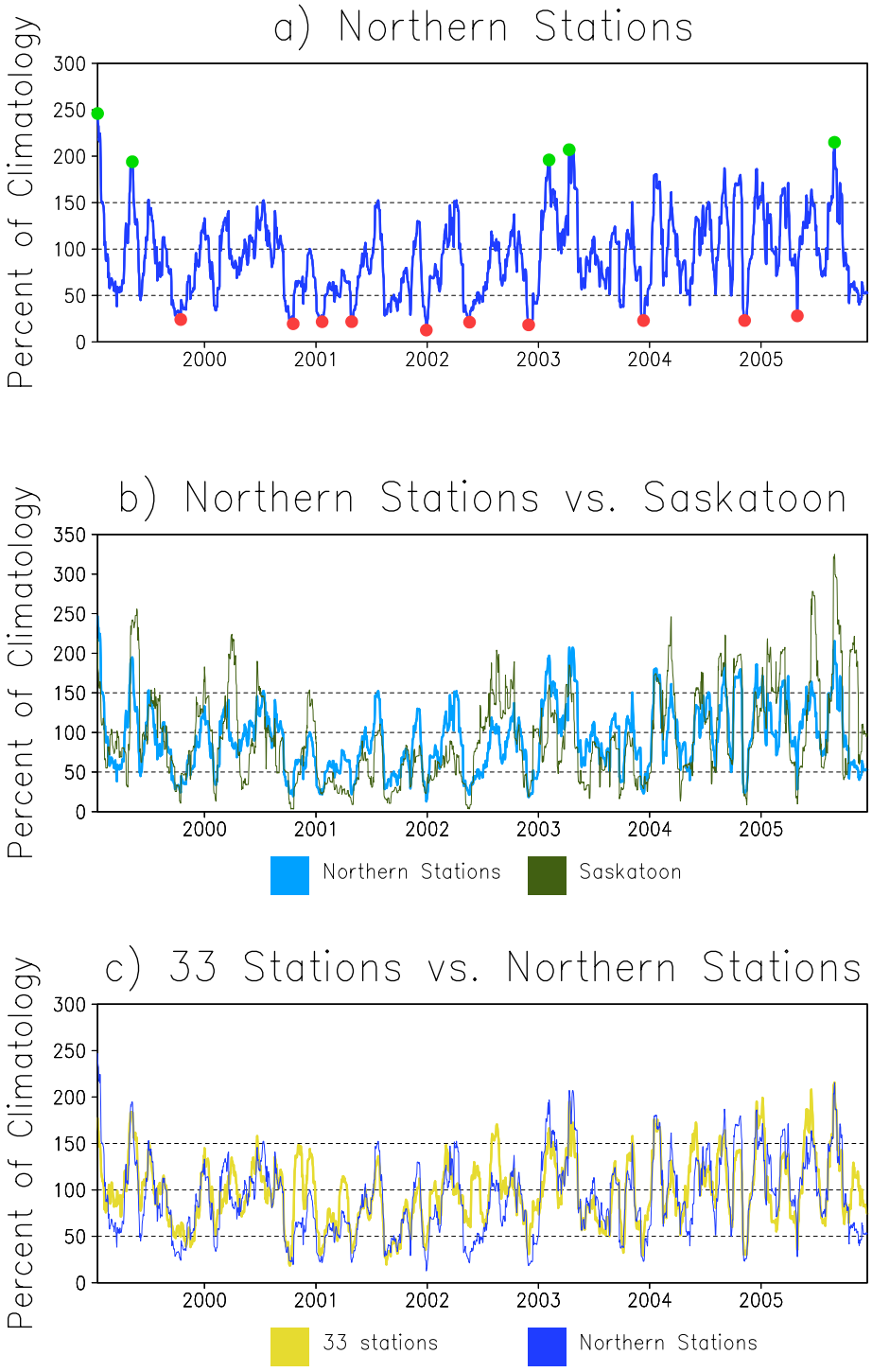

Figure 4.8: 30-day running means for percentage of climatology of precipitation for a) the northern stations, b) Saskatoon compared to the northern stations, and c) the 33 stations compared to the northern stations. The red and green points in a) are the identified key severe dry and wet periods, respectively (i.e. lowest ten and top five values).

Table 4.2: Wet Events: Top 5 values of a) northern station time series and b) the 33-station time series. The northern station wet events are denoted in green in Fig. 4.8a. The * indicates an identified key period that is unique to the northern stations.

(a) Northern Stations

Central Date	30-day percentage
1) 15 January 1999*	246.92%
2) 30 August 2005	215.54%
3) 12 April 2003	207.29%
4) 5 February 2003*	196.96%
5) 9 May 1999	194.85%

(b) 33 Stations

Central Date	30-day percentage
1) 30 August 2005	215.86%
2) 15 June 2005	208.23%
3) 6 January 2005	199.39%
4) 13 April 2003	195.52%
5) 9 May 1999	183.99%

The severe "drought signature" is easily distinguished in a single station such as Saskatoon (green in Fig. 4.8b) as the peaks and troughs are much more extreme. In particular, the 30-day running means for Saskatoon remain below 100% from January 2001 to mid June 2002 for all but a few 30-day periods centred at the end of July 2001. As Saskatoon is one of the 11 northern stations, it is not surprising that the maximum and minimum values for the northern station curve match very well to those in the curve for Saskatoon in Fig. 4.8b.

As seen in Fig. 4.8c, the 30-day running means for the northern stations (blue) compare well to the full 33-station average (yellow). The correlation between the two time series is quite high (0.80). There are two main areas, however, where the Northern station curve deviates from the 33-station curve – autumn 2000 to spring 2001 and the growing season of 2002. In autumn 2000 to spring 2001, the three minimum points occur simultaneously in both curves, but the peaks are slightly enhanced in the 33-station curve. This indicates that the severe periods of the drought from autumn 2000 to spring 2001 occurred simultaneously in both the north and south of the Prairies, but was slightly more enhanced in the northern part, consistent with the spatial representation in Fig. 4.5. However, during the growing season of 2002, the two curves are slightly out of phase, with a minimum in the northern stations and a maximum in the 33-station average around the same time. This represents the high-low precipitation couplet in the 2002 growing season, as shown previously in Figs. 4.5, 4.6, and 4.7. It was found that eight out of the ten dates identified as dry events and three out of five wet events from the northern subset of stations were in common to those from the full 33-station average,

albeit in an altered order (see Table 4.1b and 4.2b). Here, "common" means that the 30-day periods overlap, i.e. the central dates are within 15 days of each other. The relative consistency of the identified extreme events from the northern station and 33-station curves gives confidence to this methodology and robustness to the results in the following section.

The two dry events that are unique to the northern subset of stations, 20 May 2002 and 15 October 1999, are noteworthy. The first is during the growing season of 2002, which, as mentioned above, was characterized by the high-low percent normal of precipitation couplet (see Figs. 4.5b, 4.6, and 4.7). The fact that the northern station time series captures this May 2002 event further justifies the use of this subset of stations for the identification of the dry periods. October 1999 is significant in the sense that autumn 1999 was characterized by extreme west coast precipitation and continental dry conditions and can be considered the "kick-off" of the drought.

4.3 Synoptic and planetary analysis of key dry periods

Despite its importance, there is an inherent difficulty in studying a long timescale feature (drought) using synoptic-scale fields. As mentioned above, this issue was addressed by taking a 30-day mean of the synoptic fields, as a compromise between the two temporal scales. This method is not without fault, however. It should be noted that the fields presented can be smeared if the signal is weak or if there is large variability in the pattern throughout the 30-day period. This additional smearing issue was addressed by also analyzing time-height cross sections and atmospheric soundings, which effectively show the variability about the 30-day period.

An approximate Eady model (Eady 1949) representation (i.e. upper-level 300 hPa and surface MSLP) of the key dry events as defined in Table 4.1a of the previous Section is given in Fig. 4.9. It was found that the dry events can be arranged, or loosely typed, according to the dominant subsidence mechanism, and thus flow

Table 4.3: Dry events and their corresponding mechanisms. Parentheses indicate secondary mechanisms which cannot cannot be seen in the 30-day mean fields. Dry rankings refers to the 30-day mean percent normal (from Table 4.1)

Central Date	Dry Ranking	AVA	CAA	Downsloping
Case A: 29 December 2001	1	✓	(✓)	
Case B: 30 November 2002	2	✓	(✓)	
Case C: 21 January 2001	5	✓	(✓)	
Case D: 12 December 2003	7	✓	✓	(✓)
Case E: 30 April 2005	10	✓	✓	
Case F: 20 May 2002	4	✓	✓	
Case G: 18 October 2000	3	✓		✓
Case H: 8 November 2004	8	✓	(✓)	✓
Case I: 28 April 2001	6	(✓)	✓	✓
Case J: 15 October 1999	9	✓	(✓)	✓

regime. As mentioned in Section 3.3, there are three important subsidence mechanism for the Prairies. From the QG omega equation (Equation (3.6)), the synoptic-scale mechanisms for subsidence are AVA and CAA. The third subsidence mechanism, downsloping, is related to the boundary condition (terrain, Rocky Mountains), and thus has a much smaller scale influence than the QG mechanisms. Most of the events are in fact associated with not one, but a combination of these mechanisms, and are listed generally in the order from large-scale to small-scale subsidence regimes in Table 4.3. This order roughly corresponds to the flow regimes of large-scale ridging (Fig. 4.9a–f) to a greater zonal and downsloping component (Fig. 4.9g–j). The events will be discussed in this order in the following sections. It should be noted that the parentheses in Table 4.3 denote weaker, or secondary mechanisms which cannot be easily seen in the 30-day mean fields alone. The time-height cross sections and soundings (in the downsloping cases) provide the additional detail needed to further determine the subsidence mechanisms which are not as evident in the 30-day averages. These time-height cross sections are from Saskatoon, Saskatchewan (CYXE, #25 in Fig. 3.1). The fact that the cross section is taken at a single point does not hinder the results, as a time-height cross section approximates an east-west cross section for synoptic-scale features travelling eastward through the station. Saskatoon was chosen as it is located approximately in the middle of the study region, and was particularly affected by the drought

as seen in the percent normal precipitation 30-day running means in the previous section (Fig. 4.8b). Daily PNA is also included in the Fig. 4.9 to orient the events in terms of the planetary scale.

4.3.1 AVA dominant cases

Cases A–D (Figs. 4.9a–d), all winter cases, are clearly dominated by persistent positive PNA ridging in western North America. This in fact agrees with the traditional ridging paradigm for Canadian Prairie drought as suggested by Dey (1982). The ridge is weaker and less evident in Case D (Fig. 4.9d); however, the persistent positive, yet weaker, PNA signal gives confidence in grouping Case D with A–C. Undoubtedly, some smearing is occurring which drowns out some of the ridge signal in Case D. Nevertheless, in Figs. 4.9a–d, the ridge axis is centred along the West Coast (British Columbia, BC), which corresponds to a vorticity minima due to strong anticyclonic curvature. In this regime, the Prairies are downstream of the ridge axis, and thus are in an expansive region of AVA advected by the northwesterly flow aloft. This sets up, through the differential advection term of the QG omega equation (Equation (3.6)), a broad region of descent (subsidence) and adiabatic warming in the region of AVA. The associated surface divergence leads to anticyclogenesis, as seen by the surface high pressure system in northwestern US, with an inverted ridge creeping into the southern Prairies. Both the upper-level and surface ridges deflect storms poleward, preventing entry into the Prairies. The surface trough extending from the cyclone in the Gulf of Alaska into northern Canada (Fig. 4.9a–d), which in a 30-day mean, represents a storm track, shows this northward deflection of storms. Case C differs slightly from A and B in that there is evidence of an upper-level trough in the southern stream near California which supports the idea of a split flow, deflecting storms to both the north and south of the Prairies. In addition, owing to the more zonal upper- and surface flow in Case D, downslope flow is also present.

Of great interest is the strong cyclone in the Gulf of Alaska in all four cases, which, in conjunction with the continental high pressure system to the southeast,

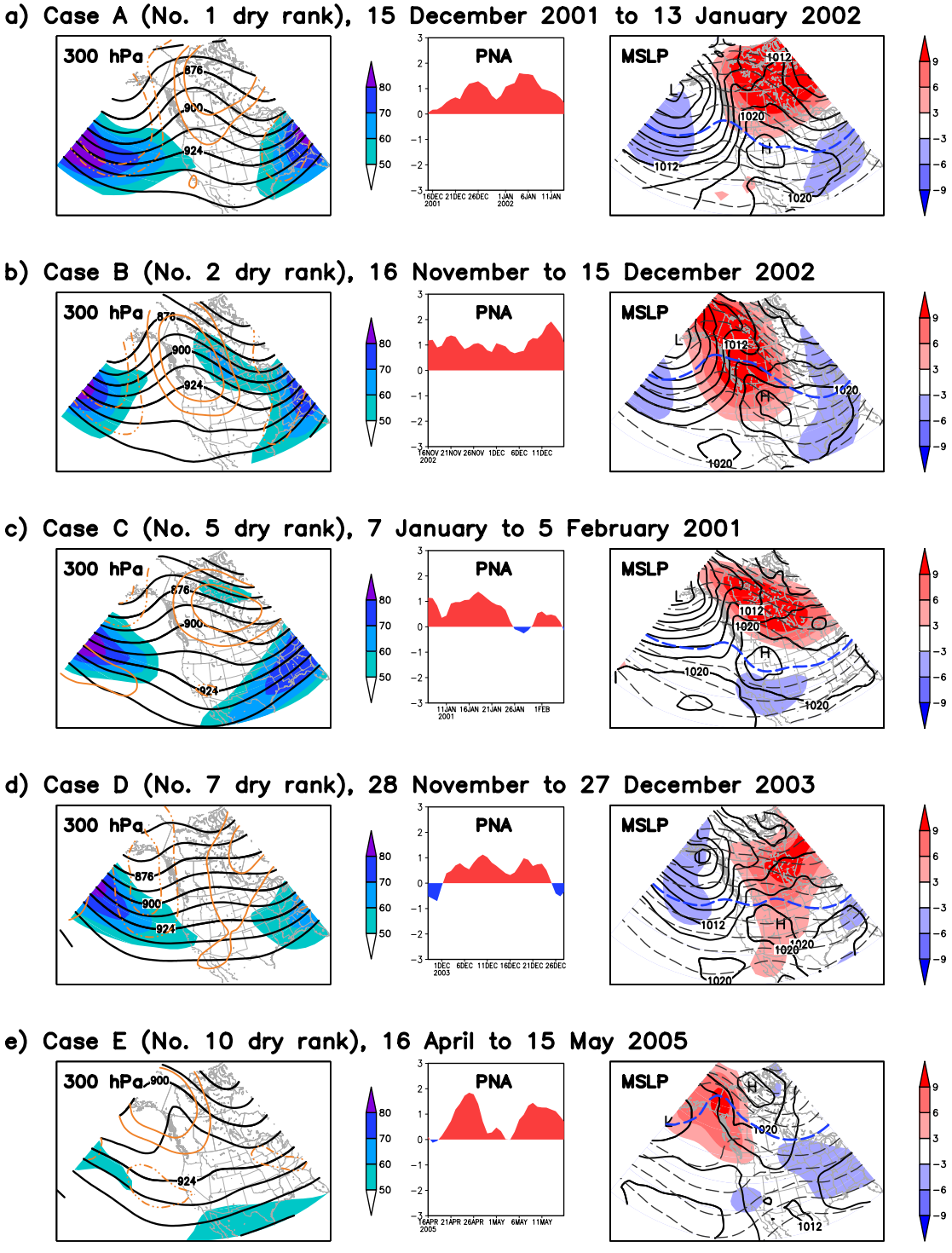

Figure 4.9: a)–e) Dry Cases A–E. Left panels: 30-day averages of 300 hPa heights (dam, black contour, 12 dam interval), 300 hPa height anomalies (dam, orange contour, solid is positive), and isotachs (kts, shaded). The ±6 and ±12 dam contours are shown for the height anomalies. Right panels: 30-day averages of MSLP (hPa, solid, 4 hPa interval), 1000-500 hPa thickness (dam, dashed, 6 dam interval), and thickness anomalies (dam, shaded). PNA is shown in the middle.

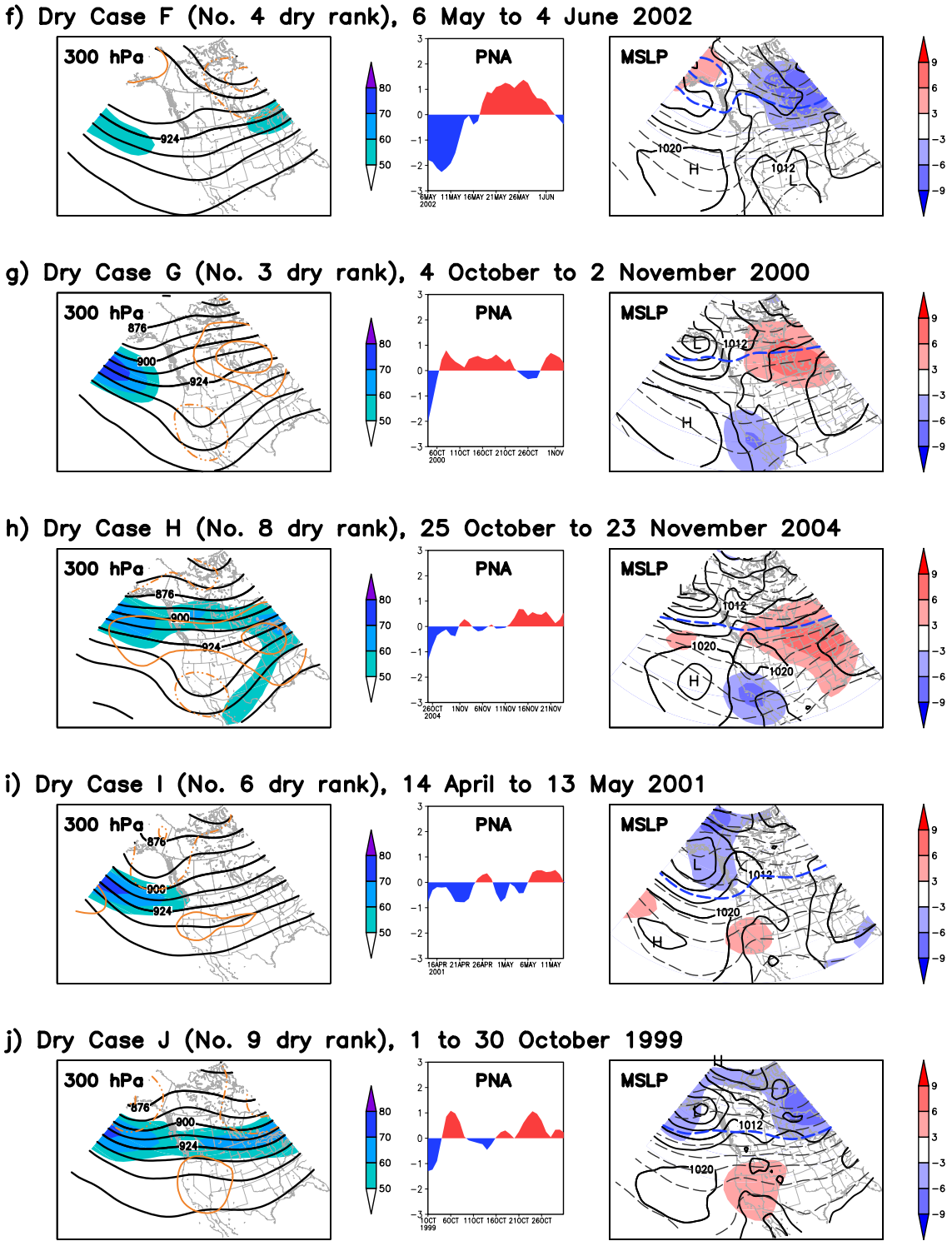

Figure 4.9: f)–j) Dry Cases F–J.

produce very strong southerlies off the coast of BC (Fig. 4.9a–d). Prior studies have shown that Gulf of Alaska cyclones and associated IWVT enhance downstream ridging (in the Prairies) through WAA and diabatic effects due to latent heat release from precipitation (e.g. Roberge et al. 2009). Indeed, not only do the surface southerlies in Cases A–D transport moisture northward off the coast of BC (e.g. 700 hPa for Case B in Fig. 4.10a), but are also responsible for large amounts of southerly WAA in the same area, impressive for a 30-day mean (Fig. 4.9a–d). The WAA creates a thermal ridge in this area (see 540-dam thickness contour in Figs. 4.9a–c). By the QG height tendency equation (Bluestein 1992), the WAA and enhances the downstream height ridge, represented by the positive height anomalies in the ridge axis (Figs. 4.9a–d). In turn, these anomalously positive heights increase the AVA and adiabatic warming due to subsidence, thus leading to the creation of the anomalously warm thicknesses that engulf most of western Canada in cases A–D. The fact that Cases B and D (Figs. 4.9b and d) correspond to the 25 November 2002 and 18 December 2003 IWVT events found in Roberge et al. (2009) supports the conclusion that IWVT events in the Pacific impact Prairie drought (Roberge et al. 2009).

Despite the intense WAA off the coast of BC, temperature advections over the Prairies are minimal in Cases A–D, as shown by the equivalent barotropic signature in the 30-day MSLP and 1000–500 hPa thickness means (Figs. 4.9a-d). However, the cross sections show that CAA is also present, particularly in Cases A (see Fig. 4.11a) and D (not shown), which aids the AVA as a subsidence mechanism. Figure 4.11a shows that CAA and AVA give long-lived subsidence around 1 January 2002 (denoted by the purple box). AVA, however, is the more effective mechanism for descent in Fig. 4.11a, even in periods of WAA (e.g. 6–11 January 2002, purple box), whereas CAA alone does not generate descent (e.g. 3–4 January 2002, purple box). Thus, the dominant subsidence mechanism in the winter Cases A–D is AVA due to anticyclonic curvature (ridging). CAA also acts as a weaker, secondary mechanism, particularly in Cases A and D, and downslope flow is also a secondary subsidence mechanism in Case D. It is of note that three out of the driest five cases (from Table

4.1a) are associated with this large-scale ridging regime, indicating that this is still the most effective regime for subsidence and drought in the Canadian Prairies.

4.3.2 CAA dominant cases

Cases E and F (Figs. 4.9e–f), which both occur in spring, have some resemblance to Cases A–D in their upper-level ridge pattern and northwesterly flow. Thus, it can be concluded that one mechanism for subsidence in Cases E and F is the associated AVA owing to anticyclonic curvature. However, since the ridge pattern, the northwesterly flow, and thus AVA, is not as strong in Cases E and F, it can be deduced that there must be another subsidence mechanism (namely CAA) that plays a larger role. The ridge in Case E (Fig. 4.9e) is rather sharp in only one contour at the 300-hPa level, but is more developed at the 700-hPa level (not shown). The western Canadian ridge in Case F (Fig. 4.9f) is weak, and the upper-level pattern resembles the split flow (i.e. diffluent 300-hPa geostrophic winds on the ridge axis) in Case C (Fig. 4.9c). Whereas Cases A–D were dominated by strong positive PNA that persistent through most of the 30-day period, the PNA in Cases E and F can be divided into two sections wherein the PNA value approaches zero in the middle of the 30-day period. In Case E (Fig. 4.9e), the two distinct periods of the PNA are both strongly positive. However, in Case F (Fig. 4.9f), the first half of the 30-day period is dominated by a strongly negative regime, then shifts to strongly positive in the second half of the period. The regime shift in Case F potentially raises the likelihood for smearing in the 30-day mean fields.

Another striking difference from Case A–D is the extremely weak upper-level flow in the Gulf of Alaska in Cases E and F as indicated by the absence of 300-hPa height contours in that region (Figs. 4.9e–f). In fact, Case E even has anomalous weak westerly flow off of the Pacific into western Canada, which is associated with the negative 300-hPa height anomaly to the west of California and the positive height anomaly over Alaska and the Yukon. This weak upper-level flow in the Gulf of Alaska leads to a confluence of height contours east of the Prairies, effectively deflecting storm tracks through the stronger southern stream and then

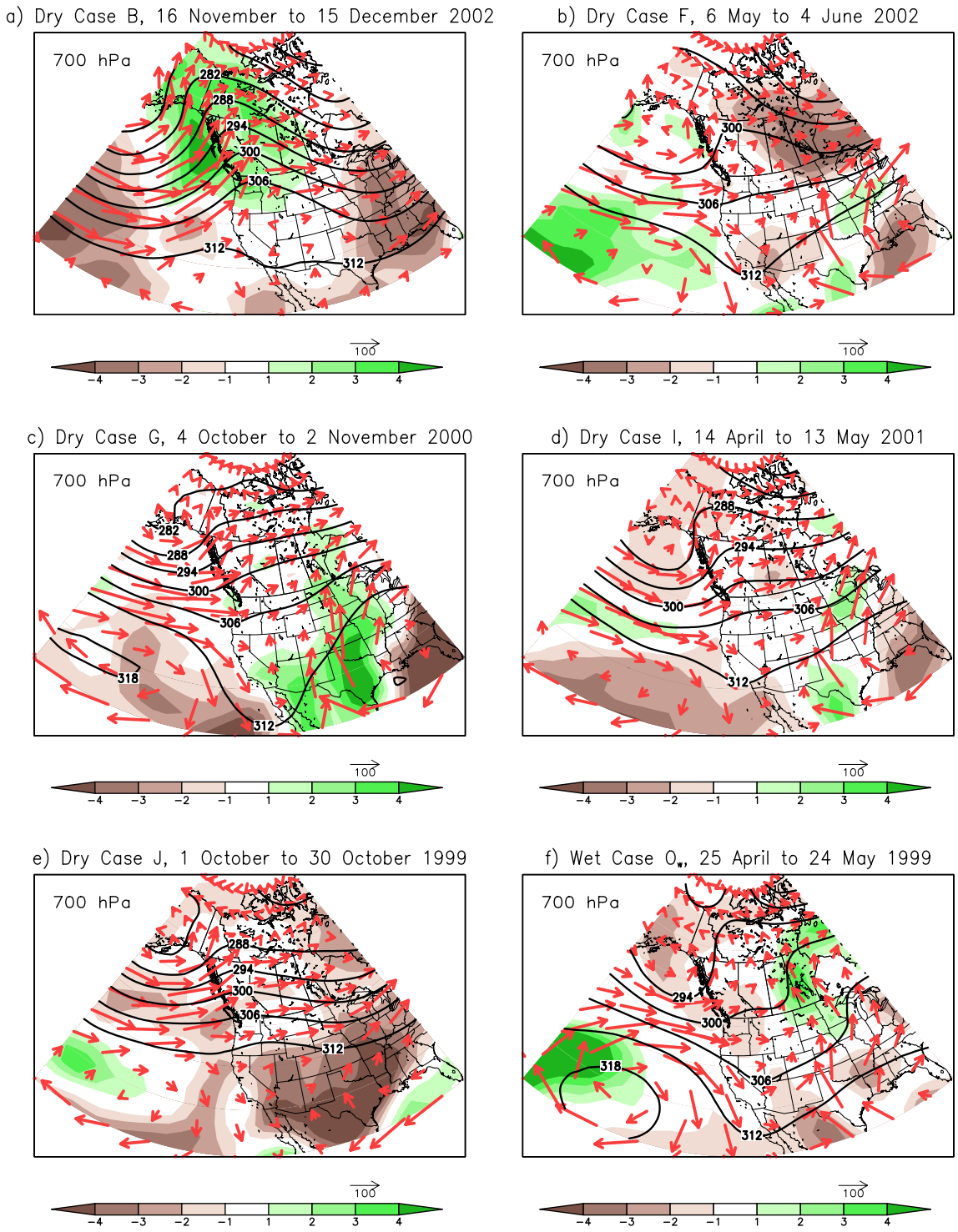

Figure 4.10: 30-day averages of 700 hPa geopotential heights (dam, solid, 6 hPa interval), precipitable water anomalies (mm, shaded) and 1000-700 hPa moisture transport (kg m^{-1} s^{-1}, arrows) for a) Case B, b) Case F, c) Case G, d) Case I, e) Case J, and f) Case O$_w$.

northeastward, thus avoiding the Prairies.

The most notable difference that makes Cases E and F unique is the association of these events with strong CAA and anomalously cold thicknesses over the Prairies (Figs. 4.9e–f). In Case E (Fig. 4.9e) the AVA associated with the upper-level ridge leads to surface divergence and anticyclogenesis downstream of the ridge axis, as evident by the high pressure system in the Northwest Territories and the associated inverted surface ridge into the Prairies. Accompanying the high pressure system in Case E (Fig. 4.9e) is very strong northeasterly CAA into the Prairies, driving a thermal trough along the Manitoba-Ontario boarder. By the QG omega equation (Equation (3.6)), CAA forces subsidence, and thus dry conditions. This CAA is shown particularly well in the cross section Case E (Fig. 4.11b). Here, CAA is a more effective subsidence mechanism than AVA around 21 April 2005 (purple box), where CAA is strong enough to generate descent even under a region of CVA. CAA and AVA are in phase around 11 May 2005 (Fig. 4.11b), and are both associated with the descent at this time. It should be noted that the AVA in Case E (Fig. 4.11b) is not as dominant as in the cross section for Case A (Fig. 4.11a). The relatively weak flow and blocking of systems is also represented in Case E's cross section (Fig. 4.11b) by the overall lack of activity and small amount of synoptic-scale forcing as compared to that for Case A (Fig. 4.11a).

The CAA in Case F (Fig. 4.9) is not as evident in the 30-day mean as it is in Case E, owing to the potential smearing of the signal. However, Case F is especially notable because it occurs during the growing season of 2002, which was characterized by the above-below normal precipitation couplet (see Figs. 4.5b, 4.6, and 4.7), in which the drought conditions were skewed northward (i.e. this was an event captured in the northern station 30-day running means, but not in the 33-stations average, see Table 4.1). Surface northwesterlies associated with the inverted surface ridge in north-central Canada in Case F (Fig. 4.9f) leads to a broad region of CAA in the Northwest Territories down into Saskatchewan, Manitoba and Ontario. What is even more striking is the large extent of the cold thickness anomalies (Fig. 4.9f) and negative precipitable water (PW) anomalies (Fig. 4.10b) in the same

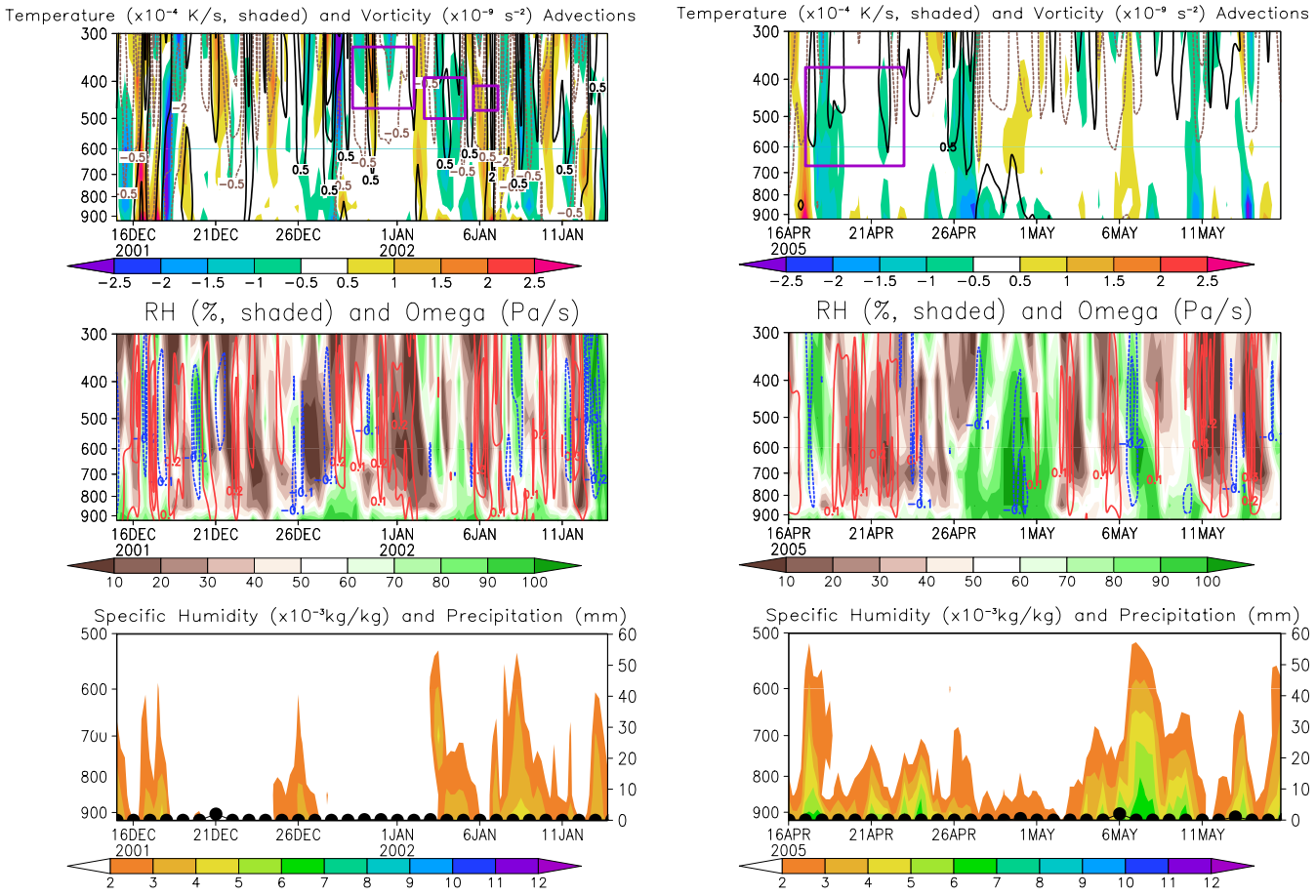

Figure 4.11: Cross Sections at CYXE for a) Case A and b) Case E. Top panel: temperature advection (x10^{-4} K s^{-1}, shaded) and vorticity advection (x10^{-9} s^{-2}, contour, black solid is CVA). Middle panel: Relative Humidity (RH, %, shaded) and omega (Pa s^{-1}, contour, dashed blue is ascent). Bottom panel: specific humidity (x10^{-3} kg kg^{-1}, shaded) and CYXE precipitation (mm, black points, scale on RHS). Purple boxes denote dates that are referred to in the text.

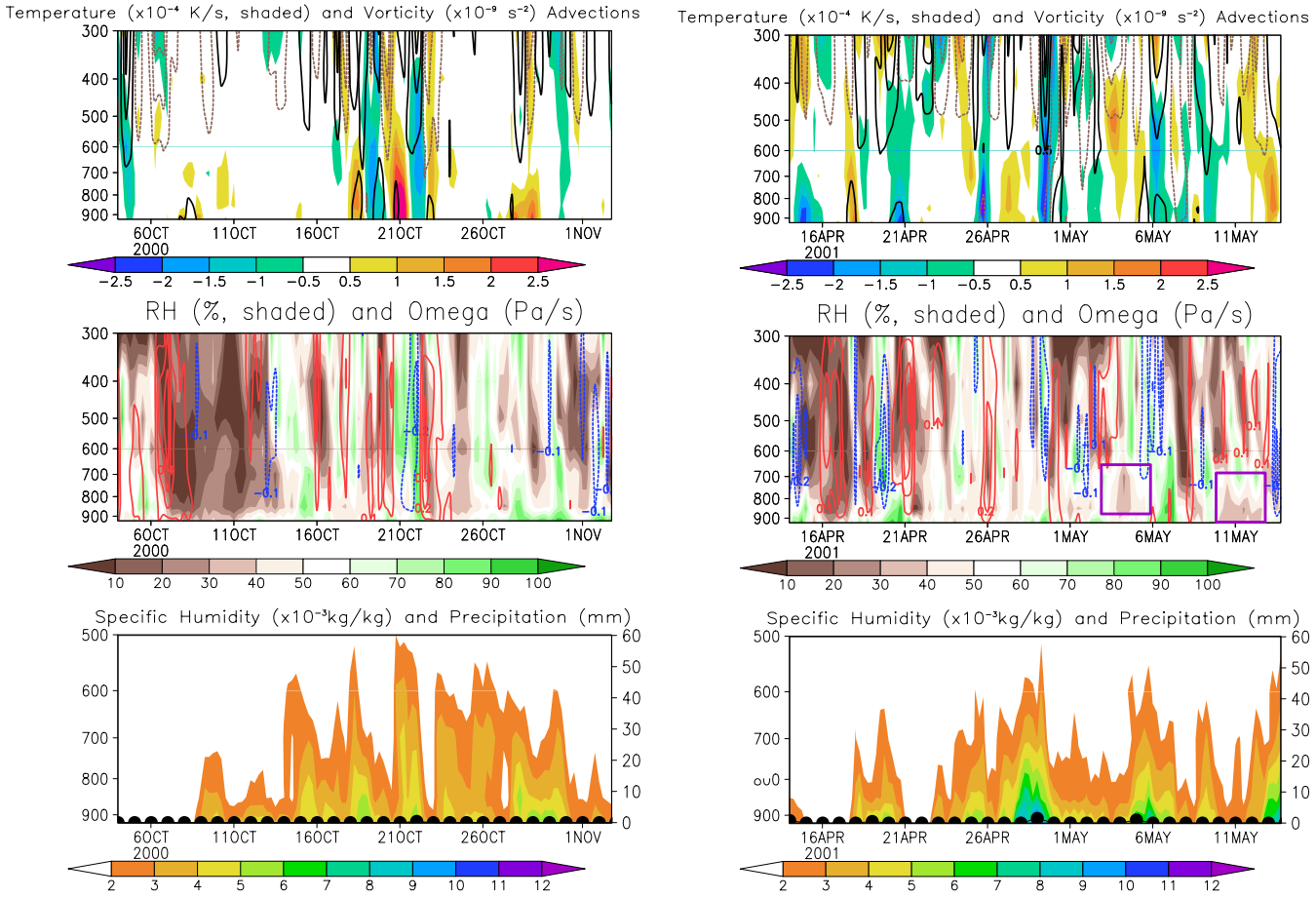

Figure 4.11: Cross Sections for c) Case G and d) Case I. Purple boxes denote dates that are referred to in the text.

region. The above normal precipitation in the southern Prairies in Fig. 4.5b seems surprising when the negative thickness and PW anomalies extend over the southern Prairies. However, a possible reason for the above normal precipitation in the southern Prairies in this case can be seen in the MSLP field in Fig. 4.9f. The 300-hPa trough in the southern stream generates CVA downstream of the axis near Texas and associated ascent and surface convergence, evident by the surface low pressure system in that location. The accompanying southerly WAA and moisture transport (Fig. 4.10b) off the Gulf of Mexico northward into the Great Plains drives a thermal ridge south of the CAA-induced thermal trough, and thus an area of frontogenesis just south of the Prairies (Fig. 4.9f). The southern Prairies catch the northern edge of the systems travelling in this southern stream.

Thus, both CAA and AVA act as subsidence mechanisms in the cold spring Cases E–F. However, CAA appears to be the more effective mechanism in these cases because of the the apparent correlation between CAA and descent in the cross sections.

4.3.3 Downsloping dominant cases

Cases G–J are markedly different from Cases A–F. Specifically, Cases G–J have an average zonal geostrophic wind of 50 kts (over 30 days) at 300 hPa over the Prairies as opposed to 35 kts (over 30 days) in Cases A–F, an increase of approximately 50% (Figs. 4.9g–j). As discussed in Section 3.3, zonal upper-level flow over the Rocky Mountains leads to forced ascent and surface divergence on the windward side, and downslope flow (descent) and surface convergence on the lee side. Therefore, the increased zonal component of the upper-level wind in Cases G–J indicates that downslope flow has a greater role in generating the subsidence in these cases. Additionally, Cases G–J are characterized by a fluctuating PNA with no persistent or strong signal, in contrast to the persistence and strength in Cases A–F. This group can be additionally separated into two sub-groups – Cases G–H and Cases I–J – based on slight variations in the structure of their upper-level flow.

Cases G–H: Split flow

Cases G–H (Figs. 4.9g–h), both occurring in autumn, are distinguished by their upper-level split flow regime: a trough in the southern stream restricted to the US and remarkably zonal flow in Canada. The zonal northern stream leads to strong downslope flow into the Prairies and the southern stream deflects storms to the south (cf. northward displacement of storms in Cases A–D). The split flow is easily seen in the moisture transport for Case G (Fig. 4.10c), in which the transport is predominantly northerly at the West Coast, opposite of the southerly transport in the ridging Cases A–D (Fig. 4.10a). Surprisingly, this split flow regime also establishes AVA into the Prairies. However, unlike the ridging Cases A–D in which the anticyclonic vorticity was due to curvature, the AVA in Cases G–H (Figs. 4.9g–h) is attributed to anticyclonic shear. The diffluent 300-hPa contours in northwestern US (Figs. 4.9g–h) lead to weak flow south of the strong westerly flow in the Prairies, thus clearly substantiating anticyclonic shear vorticity and AVA into the Prairies. The anticyclonic shear is perhaps even more evident in Case H (Fig. 4.9h), with the elongated jet zone and the structure of the 300-hPa height anomalies. In Case H, the elongated positive 300-hPa height anomaly bounded on the north and south by negative anomalies point to an anomalous easterly in northwestern US and an anomalous westerly north of the Prairies, thus leading to anomalous anticyclonic shear vorticity and AVA into the Prairies. On the other hand, Case G has weaker shear vorticity, but the trough is deeper and more well defined (Fig. 4.9g), even at the 700-hPa level (Fig. 4.10c). This indicates that the flow in Case G is more effective at deflecting storms south and leads to the absence of synoptic activity in the Prairies as seen in the Case G's cross section (Fig. 4.11c).

The split flow is also evident in the thickness field, with completely zonal contours in the north, and a thermal trough and cold thickness anomalies near California associated with the northerly CAA in Figs. 4.9g–h. The Prairies, however, are on the western edge of a region of anomalously warm thicknesses, which are associated with weak southerly WAA evident in both Cases G–H from the Gulf of

Mexico. There is even a suggestion of CAA in southern Alberta in Case H (Fig. 4.9), which is additionally seen in the cross section for the same period (not shown). It is also interesting to note that there is in fact southerly moisture transport from the Gulf which brings in anomalously high moisture onto the continent in the southern stream, an important moisture source for precipitation generation in the Prairies. However, the strong westerly flow in the northern stream helps to deflect the moisture east of the Prairies, and the subsidence owing to downsloping and AVA in the Prairies inhibit generation of precipitation despite the moisture transport from the Gulf.

The surface systems in Cases G and H also aid in establishing downslope flow into the Prairies. In Cases G–H (Figs. 4.9g–h), a high pressure system is located directly south of the Gulf of Alaska low, aligning and enhancing the westerly surface flow off the Pacific where the systems meet near the Canada-US border. This two-system enhanced westerly surface flow intensifies the downslope flow, and thus subsidence in the Prairies. A slight change in the placement of the surface high relative to the Gulf of Alaska low appears to be significant for the subsidence mechanism involved. As opposed to the enhanced westerlies here in Cases G–H, the high pressure system was displaced southeast of the Gulf of Alaska low in Cases A–D (Fig. 4.9a–d), enhancing southerly flow off the coast.

It should be noted that this zonal-trough split flow regime is very effective in bringing about subsidence and dry conditions – Case G is the third driest 30-day period in 1999–2005 and the only case in the driest 5 (from Table 4.1a) that is not dominated by large-scale ridging. Therefore, in the split zonal flow regimes of Cases G–H, downslope flow and AVA due to shear vorticity are the two main mechanisms for subsidence, with CAA also playing a minor role in Case H.

Cases I–J: Zonal

Cases I and J (Figs. 4.9i–j) are related to Cases G and H in the highly zonal component to their upper-level structures. However, Cases I and J show zonal structure for the entire continent, rather than only in the northern stream of a split flow

regime (Figs. 4.9i–j). For this reason, downsloping plays a much greater role as the subsidence mechanism in Cases I and J . These two cases are also special – Case I is a critical growing season in the core of the drought (2001), and Case J is the second case that was unique to the northern stations (see Table 4.1a). Like Cases G and H, the upper-level and surface flow in Cases I and J promote westerlies, which, on the leeward side of the mountains, yields subsidence and surface convergence. Both Cases I and J (Figs. 4.9i–j) also have a slight upper-level trough in the Gulf of Alaska, unlike Cases G and H. Case I (Fig. 4.9i) mimicks the surface pattern of Cases G and H, with the strong surface westerlies off of the Pacific from the coupled effect of a strong Gulf of Alaska low and a high south of it, as well as the southerly moisture transport and WAA from the Gulf of Mexico into Central US (Fig. 4.10d). Case I, however, is a much clearer example of downslope flow – the surface pressure gradient in Fig. 4.9i is perpendicular to the terrain, the surface signature of downslope flow. Even the PW anomalies at the 700-hPa level for Case I (Fig. 4.10d) clearly show the small scale extent of downsloping through the small isolated region of negative PW in central Alberta and Saskatchewan. Additional evidence of the dominance of downsloping as the subsidence mechanism in Case I is shown by soundings during the 30-day period (Fig. 4.12) from Stony Plain (CWSE), just west of Edmonton (#7 in Fig. 3.1). These are classic downsloping soundings, as evident by the strong westerly winds aloft and the adiabatic warming and drying from 700 hPa (the approximate level of the mountain top) to the surface. These five soundings (spaced about five days apart), although they have the same signature, are show in order to demonstrate that downsloping occurred throughout the entire 30-day period. What is more surprising is the dominance of this sounding signature throughout the 30-day period – only a few soundings at 0000 UTC in this case do not show a downsloping signature. In fact, the 700 hPa to surface drying owing to downsloping is even evident in the cross section for Case I (Fig. 4.11d), particularly around 5 May and 11 May 2001 (purple boxes). Figure 4.11d also shows that CAA is an additional mechanism for subsidence in Case I, supported by the clear region of CAA in the western Prairies in the 30-day mean

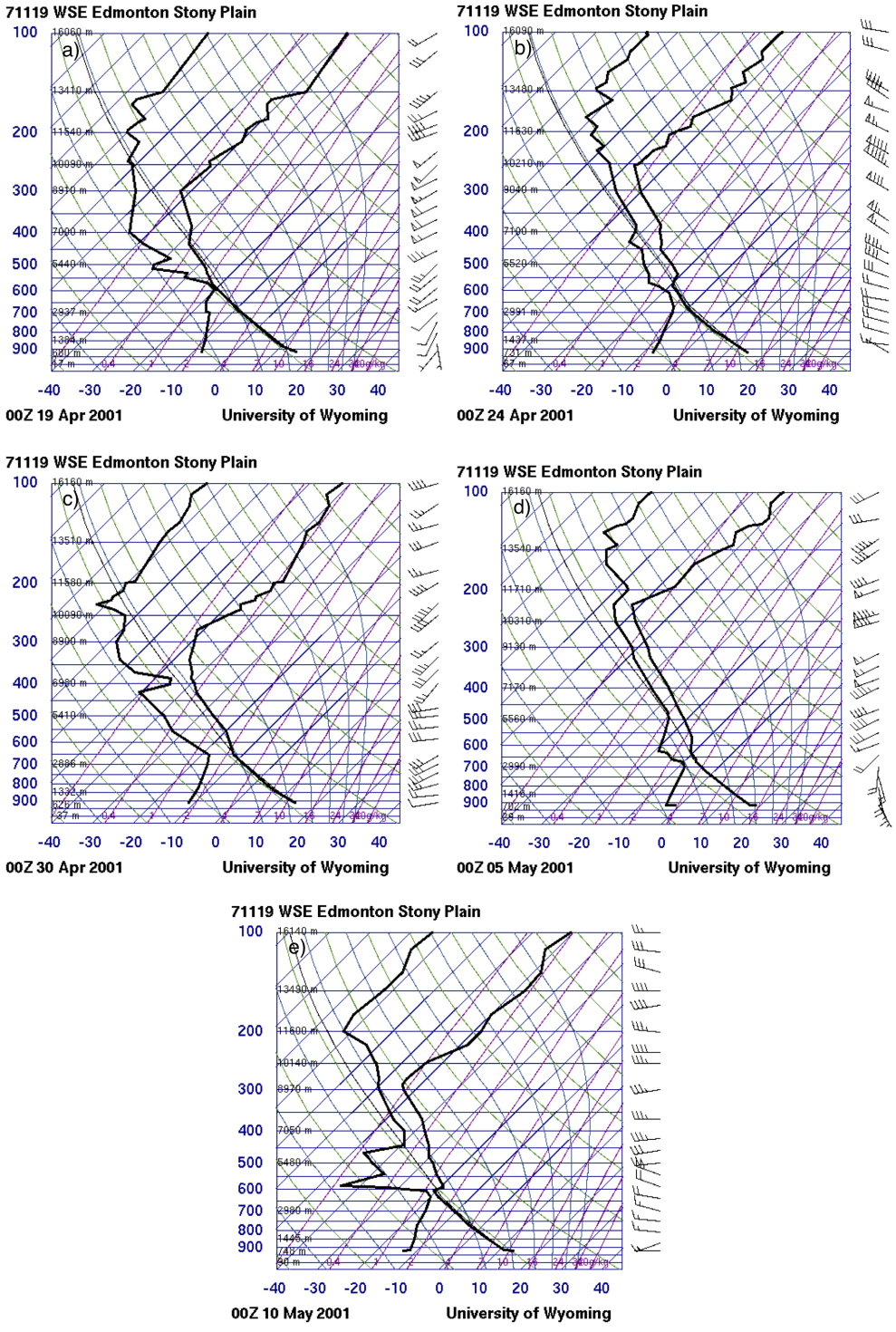

Figure 4.12: Soundings for Case I (at CWSE Edmonton Stony Plain): a) 0000 UTC 19 April 2001, b) 0000 UTC 24 April 2001, c) 0000 UTC 30 April 2001, d) 0000 UTC 5 May 2001, and e) 0000 UTC 10 May 2001.

of MSLP (Fig. 4.9i). AVA is also seen in Fig. 4.9i, but it appears that CAA is more correlated with the descent than AVA in Case I.

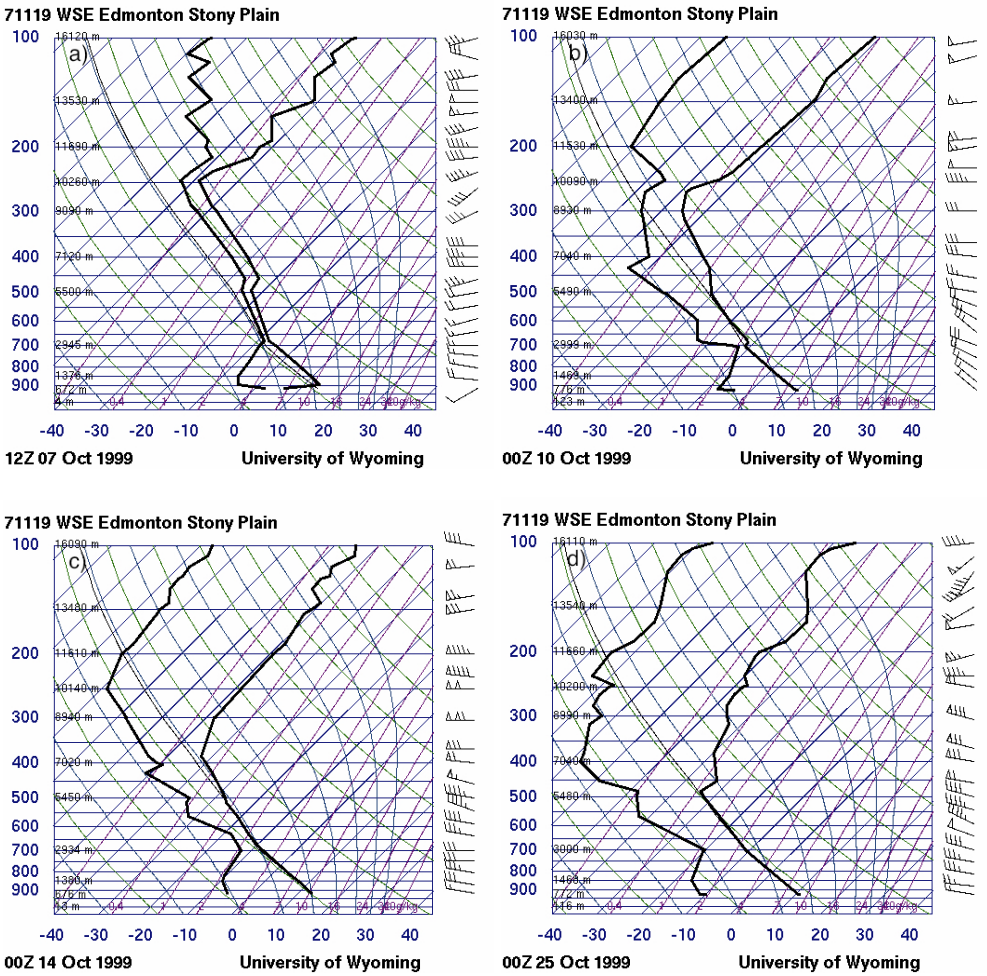

Figure 4.13: Soundings for Case J (at CWSE Edmonton Stony Plain): a) 1200 UTC 7 October 1999, b) 0000 UTC 10 October 1999, c) 0000 UTC 14 October 1999, and d) 0000 UTC 25 October 1999.

Case J (Fig. 4.9j) is very interesting because of the upper-level zonal jet band, impressive for a 30-day average. Not only are these winds very strong (greater than 50 kts), but are anomalously westerly, as evident by the positive height anomaly south of the jet, and the negative height anomalies north of the jet. Downsloping is again seen in the soundings for Case J (Fig. 4.13), but seems not to be as frequent as in Case I (although it should be noted that many soundings in this period were missing). Nevertheless, AVA, and less so CAA, also work as secondary subsidence mechanisms in Case J suggested by, respectively, the slight upper-level ridging

and a suggestion of CAA at the surface in Fig. 4.9j. Perhaps, however, the most striking depiction of this period is the 700-hPa field (Fig. 4.10e), where the the entire continent is cut off of moisture from both the Gulf of Mexico and the Pacific and is strikingly dominated by negative PW anomalies.

Thus, downsloping is the dominant mechanism for subsidence in the zonal Cases I and J, aided by AVA and CAA. This pattern is very noteworthy, and in fact, is the regime associated with August 2001, the month of apparent departure from normal in the historical perspective Section 4.1.1 (August 2001 is marked "D" on Figs. 4.1 and 4.2). This period (with a central date of 20 August 2001) is identified as the second driest event in the 33-station percentage of normal timeseries (see Table 4.1b), and is even the eleventh driest case for the northern events (not shown). The structure of the upper-level flow in August 2001 (not shown) is a hybrid of Cases I and J, having both a trough in the Gulf of Alaska (as in Case I) and a jet band (as in Case J), and the other diagnostics for August 2001 show much resemblance to Cases I and J as well (not shown). The occurrence of this zonal regime in the 33-station timeseries gives additional confidence to our methods and analysis.

4.4 Synoptic and planetary analysis of key wet periods

Following this discussion of the mechanisms of subsidence in the Prairies, the question arises as to how precipitation is actually generated in the Prairies. As a comparison to the discussion of subsidence mechanisms during the 1999–2005 drought, the top five wet events during the same period (from Table 4.2a) are examined as a further emphasis of what the key dry periods were lacking for precipitation formation.

30-day means of 300 hPa, MSLP, and PNA for the wet events are shown in Fig. 4.14. It is of note that these events occurred during the extremities of the drought period, and not during 2000–2002. In general, these wet cases can be grouped into two general ascent mechanism regimes, which also correspond to two different

seasons – troughing in the growing season and upslope flow in the winter. These cases are listed with their corresponding mechanism in Table 4.4, denoted with a "w" to distinguish wet cases from dry cases.

Table 4.4: Wet events and their corresponding mechanisms. Wet rankings refers to the 30-day mean percent normal (from Table 4.2)

Central Date	Wet Ranking	Upslope	Trough (CVA)
Case K_w: 15 January 1999	1	✓	
Case L_w: 5 February 2003	4	✓	
Case M_w: 30 August 2005	2		✓
Case N_w: 12 April 2003	3		✓
Case O_w: 9 May 1999	5		✓

4.4.1 Upslope flow

When considering the most effective precipitating systems in the Prairies, one can arguably neglect the winter cases, as the actual amount of precipitation gained in winter on the Prairies is so little compared to that received during the growing season (Bonsal et al. 1999; Dey 1982). Nevertheless, the winter wet Cases K_w and L_w (Figs. 4.14a and b) are interesting cases for winter precipitation. In fact, Case L_w (Fig. 4.14b) is under a positive PNA regime, making it reminiscent of the dry Cases A–D (Figs. 4.9a–d) which were also winter cases dominated by positive PNA. Note that the potential for smearing is heightened in Case K_w because the PNA switches sign in the middle of the 30-day period. Even so, both of the wet Cases K_w and L_w are dominated by a strong northwesterly upper-level flow over the Prairies, with Case L_w (Fig. 4.14b) characterized by an upper-level ridge axis along the West Coast thus giving it a more northerly component as opposed to the the more zonal, gentle trough along the Manitoba-Ontario border in Case K_w (Fig. 4.14a). Ridging and northwesterly flow, however, was also a characteristic of the dry Cases A–D (Fig. 4.9a–d).

The difference between these dry and wet winter cases lies in the surface pressure and thickness structure. Firstly, the main reason that Cases K_w and L_w are wet stems from the fact that both surface maps show a component of easterly flow associated with the surface anticyclone near Alberta (Figs. 4.14a and b). Easterly

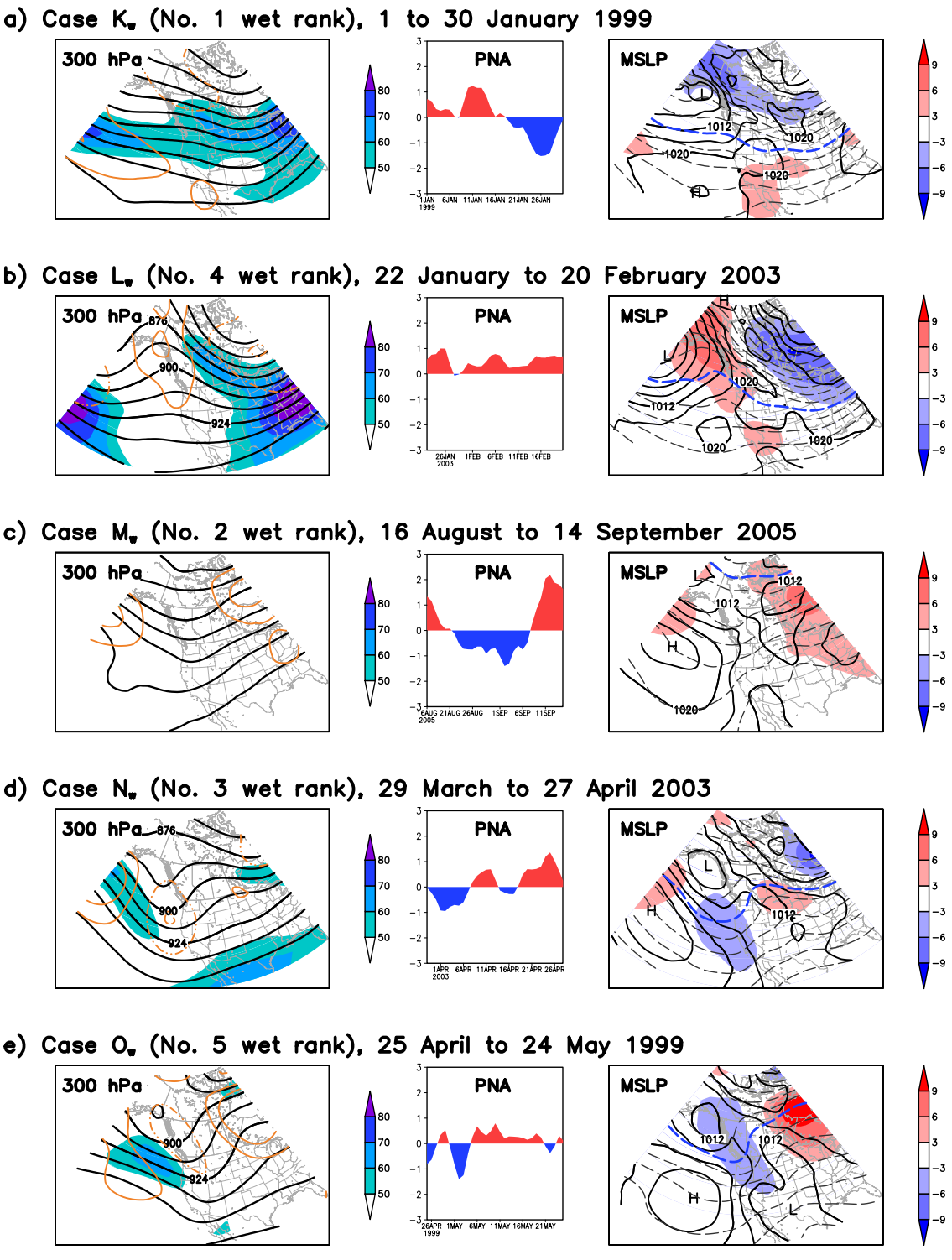

Figure 4.14: As in Fig. 4.9 but for the top 5 wet events.

surface flow in the Prairies is alone a mechanism for ascent, as it implies upslope flow (forced ascent) and associated precipitation. Second, both of these cases have a very strong baroclinic zone (potentially conducive to frontogenesis) spanning northwest-southeast across the Prairies, with cold thickness anomalies to the northeast of the Prairies. Inherent in a baroclinic zone is the potential to generate disturbances – the tight temperature gradient allows for greater temperature advections. In fact, a storm track signature (i.e. surface trough) from BC southeast to Montana is seen in both Figs. 4.14a and b, which is consistent with the baroclinic zone and indicates that the Prairies are affected by the northern end of these systems. In Case K_w, the Prairies are under a region of southeasterly WAA, which is also associated with ascent by the QG omega equation (Equation (3.6)) and thus precipitation. Temperature advections in Case L_w (Fig. 4.14b), however, are minimal over the Prairies as seen by the parallel thickness and MSLP contours in the region. This is supported by the minimal evidence of WAA in the cross sections (e.g. for Case K_w, Fig. 4.15a). Thus, the mechanism for ascent in Cases K_w and L_w is easterly upslope surface flow. Overall, however, this is a weak forcing and only generates a very small amount of precipitation, as seen in the cross section for Case K_w (Fig. 4.15a).

4.4.2 CVA (trough) regimes

The mechanism for ascent in Cases M_w to O_w (Figs. 4.14c–e) is much more effective at generating precipitation, namely CVA (see cross section for Case M_w, Fig.4.15b) cross section). Refer to both over the Prairies owing to a deep upper-level trough off of the West coast. In fact, Cases M_w to O_w are all within the growing season, and are characterized by greater accumulation than the winter cases (third panel, Fig. 4.15b vs. 4.15a). Unlike the dry cases where some west coast troughing is evident (e.g. Cases G–I, Figs. 4.9g–i), the troughs in Cases M_w to O_w are latitudinally deep enough to influence the Prairies. By the differential vorticity advection term of QG omega equation (Equation (3.6)), CVA is associated with ascent and convergence at the surface by continuity (Equation (3.7)). This is a classic pattern for placing a

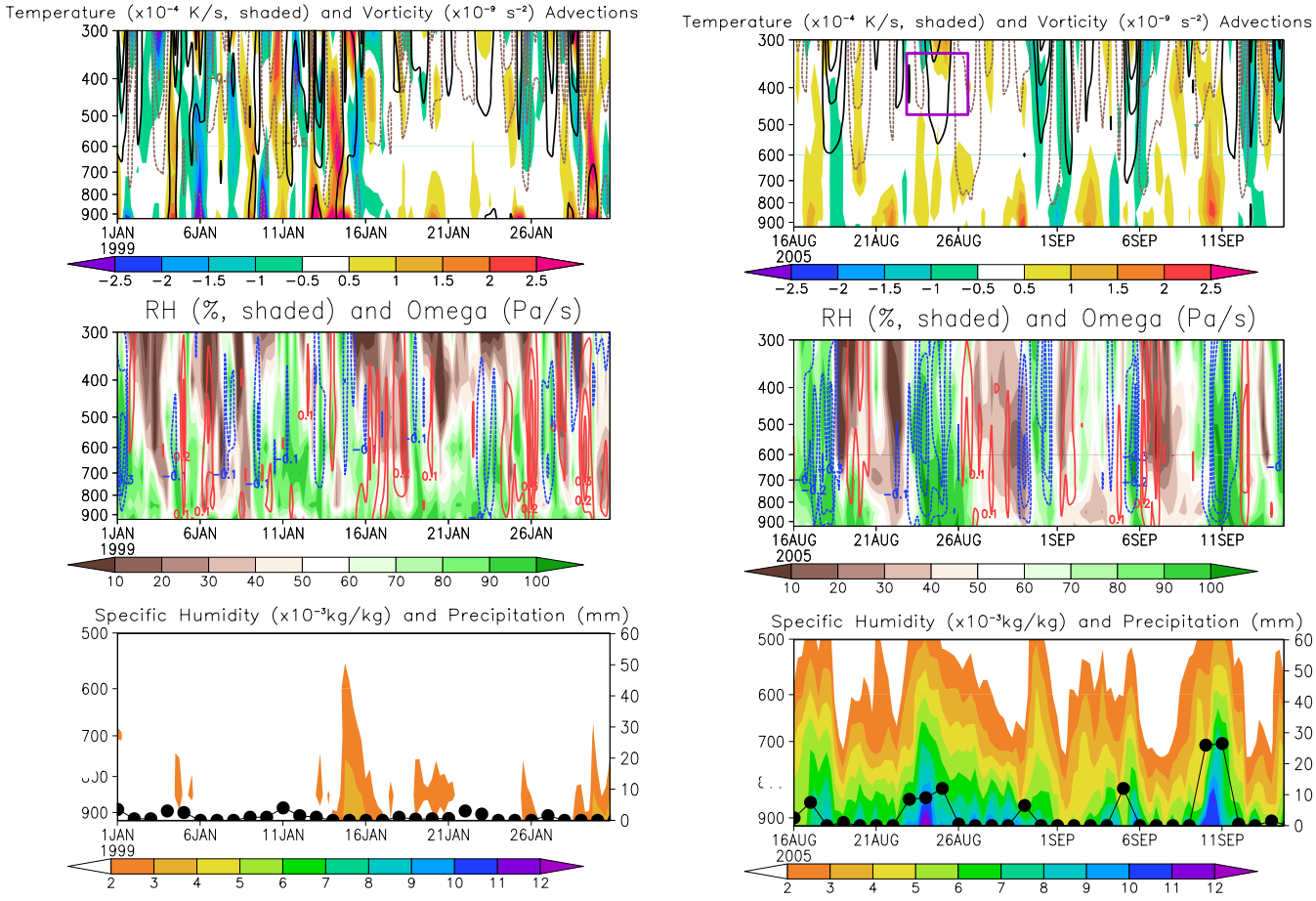

a Case K_w b Case M_w

Figure 4.15: Cross Sections for wet events: a) Case K_w and b) Case M_w. Purple boxes denote dates that are referred to in the text.

surface low in the Prairies, or centred just south of the Prairies. It should be noted that this surface low feature is not exactly obvious, but is rather suggested in the 30-day mean MSLP (Figs. 4.14c–e). For instance, Case N_w (Fig. 4.14d) shows a striking 30-day storm track (i.e. surface trough) stemming from the low in the Gulf of Alaska, continuing southeast through the western Prairies and Iowa, and eastward to Ohio. The surface trough storm track signature in Case O_w (Fig. 4.14e) appears as a trough extending northward from the low in the Gulf of Mexico area. The thickness fields give even further evidence of the surface low in the Prairies. In all three Cases M_w to O_w, the Prairies are downstream of a thermal trough, set up by CAA on the western side of the cyclone and WAA on the eastern side of the cyclone. The geostrophic surface flow from the Gulf of Mexico northwest into the Prairies in Case O_w (Fig. 4.14e) is very impressive for a 30-day mean, and allows for much moisture transport into the Prairies (see Fig. 4.10f), as is needed for growing season precipitation (Liu et al. 2004).

It is interesting to compare this 700-hPa plot for Case O_w (Fig. 4.10f) to that of dry Case G (Fig. 4.10c). Surprisingly, there is a larger region of positive PW anomalies, and seemingly stronger transports onto the continent from the Gulf of Mexico in dry Case G (Fig. 4.10c), a rather counterintuitive situation for a dry event. The paramount difference, however, lies in the direction of the moisture transports in the Prairies and the difference in synoptic-scale forcing. Whereas the moisture transports and the geostrophic flow at 700 hPa is westerly to southwesterly in Case G (Fig. 4.10c), the geostrophic flow over the eastern Prairies is more southerly in Case O_w (Fig. 4.10f) due to the latitudinally deeper trough, and the moisture transports have a slight easterly component. In addition, the trigger for ascent in the Case O_w comes from the CVA due to curvature, which is even anomalous CVA over the Prairies because of the positive 300-hPa height anomalies flanking the trough axis (Fig. 4.14e). In dry Case G (Fig. 4.9g), as mentioned above, the zonal flow and anticyclonic shear provide an extreme damper on ascent despite favourable moisture transports. This is an excellent example of the crucial necessity of a trigger for ascent, and that moisture alone is not enough to generate precipitation in the

Prairies.

It does not, however, take extreme and frequent amounts of synoptic-scale forcing to effectively generate precipitation in the Prairies. As seen in the cross section for Case M_w (Fig. 4.15b), the synoptic forcings (vorticity and temperature advections) are not as frequent as seen in some of the "hyperactive" dry cases (e.g. Fig. 4.11a). In Fig. 4.15b, we see couplings between full column ascent, saturation, and precipitation, separated by descent and subsequent drying. In terms of synoptic forcings, WAA and CVA are either coupled at the same time (e.g. before 26 August 2005, purple box), or WAA slightly precedes the CVA, which agrees with the idea that WAA precedes the centre of the low pressure (i.e. CVA). Another difference that is important to note between the cross sections for the wet and dry cases is that low-level moisture is available in the wet cases (Fig. 4.15), but is completely absent from the dry cases (Fig. 4.11).

Thus, effective precipitating systems in the Prairies occur during the growing season (April to September) and involve latitudinally deep troughs centred over the West Coast which provide CVA as a mechanism for ascent. Moisture transport from the Gulf of Mexico, with an eastward component into the Prairies, as well as low-level is also crucial in these precipitating systems. It is noted that the wet cases studied are only a small selection, and that convective systems are not completely considered here. Raddatz and Hanesiak (2008) showed that the majority of Canadian Prairie high precipitating events in 2000–2004 were convective in nature. However, despite the high frequency of these convective events, they precipitated over a much smaller area than larger synoptic systems (Raddatz and Hanesiak 2008). Thus, larger synoptic systems are undoubtedly more effective at ending meteorological drought conditions than the more frequent convective events, giving confidence to the above results. In addition, the similarities in the wet cases and the idea that convection can be inhibited if the overall synoptic conditions are not conducive to ascent gives additional confidence in these results.

CHAPTER 5

Conclusions

Drought is a very complex natural hazard, the effects of which are felt in most aspects of society and the natural environment. The impacts on society are devastating, often leading to GDP and employment loss in developed nations such as Canada, but can also lead to malnutrition and mortality in extreme cases in developing nations such as those in Africa. Its slow, nebulous nature makes it difficult to both define and measure, particularly because every drought is unique in its spatial extent, duration, and severity, and largely dependent on local climatic conditions. The study of drought can be divided into meteorological, agricultural, hydrological, and socio-economic aspects, each defined with different timescales and quantification measures (i.e. drought indices).

This study focussed on the meteorology of the assigned 1999–2005 drought period in the Canadian Prairies, the region in Canada that is most often plagued by drought. This drought caused a GDP loss totalling $5.8 billion in 2001–2002, and incurred increased amounts of forest fires (Bonsal 2008). As first noted by Bonsal and Wheaton (2005), the meteorology of this drought did not conform to traditional paradigms (i.e. positive PNA-like persistent ridging) that are common to previous droughts in the Canadian Prairies. This 1999–2005 drought was also unique in its northward extent, and lack of persistent teleconnection (Bonsal and Wheaton

2005).

This 1999–2005 Canadian Prairie drought was examined using several datasets including corrected daily and monthly precipitation station data, gridded precipitation (GPCP) and PDSI datasets, soundings, and reanalysis data. The complexity of drought was directly encountered in the attempt to identify key severe periods with the synoptic timescale in mind. Analyses of moisture divergence brought to light both an issue with the NARR (precipitation affecting mass fields) and the ineffectiveness of using this field to diagnose drought in the Canadian Prairies. A percent normal of daily precipitation technique, with a 30-day running means filter, was used to identify the ten most extreme dry and five wettest periods in 1999–2005. A subset of northern stations, as opposed to all 33-stations, was used in this identification because of the northern reaches of this drought, as particularly seen in the very interesting high-low precipitation couplet in the growing season of 2002. The two out of ten of the most extreme dry events that were identified by the northern stations but not the 33-station average (20 May 2002 and 15 October 1999) were significant periods, giving confidence to the choice of events. These key severe dry and wet periods were then analyzed using 30-day mean fields at the upper-level with 300-hPa heights and winds, and at the surface with MSLP and 1000-500 hPa thickness. The analysis was also supplemented by soundings, 30-day means of 700-hPa heights, PW anomalies, and moisture transports, as well as time-height cross sections of synoptic forcings (temperature and vorticity advections), specific and relative humidity, vertical velocity, and precipitation.

The meteorological analysis of the ten dry cases revealed four main groupings based on subsidence mechanism, or combination thereof, generally ranging from large-scale ridging to small-scale downsloping regimes. The first regime was found to agree with the traditional paradigm for Canadian Prairie drought: positive PNA ridiging in western North America, putting the Prairies in a broad region of AVA due to curvature and deflecting storms north of the Prairies. In these cases, the strong Gulf of Alaska low coupled with the continental high to the southeast drove extreme southerly WAA off the coast of BC, enhancing the downstream ridge as

suggested by Roberge et al. (2009). CAA also acts as a secondary mechanism in these large-scale ridging cases. All four events in this regime occurred in winter, and three out of the top five most extreme dry events fell into this category, leading to the conclusion that large-scale ridging and the associated AVA is still the most effective mechanism for subsidence in the Prairies, and that this regime is most prevalent in the winter.

The dominant subsidence mechanism that characterized the second dry regime was CAA, with AVA playing a much more minor role. Both of the two cases that fell into this regime were spring cases that had a severe lack of upper-level flow in the Gulf of Alaska and were marked by much less synoptic activity, in great contrast to the first ridging regime. In these cases, the amplitude of the PNA was strong but approached zero in the middle of the 30-day period.

The third and fourth dry regimes had a much greater zonal component in the upper-level flow, thus making the dominant subsidence mechanism downslope flow. In these cases, the PNA was variable and had a small amplitude. Downslope flow was aided at the surface by the positioning of a high pressure system directly south of the Gulf of Alaska low, enhancing surface westerlies off of the coast. The third regime was dominated by a split-flow upper-level structure in which a trough off of the West Coast dominated the southern stream, but was not deep enough to influence the extreme zonal flow in the northern stream. Unique to these split-flow dry cases was a secondary mechanism of AVA due to anticyclonic shear, as opposed to curvature, as well as deflection of systems mainly to the south. This split-flow downsloping regime is a very effective mechanism for drought, with one of these cases ranking just as high as the traditional ridging paradigm. The fourth subsidence regime consisted of a much more zonal component to the flow, making downslope flow the dominant mechanism, as seen by the remarkable prevalence of soundings with downsloping signatures.

The analysis of the identified wet periods during 1999–2005 revealed two different regimes: upslope flow in the winter, and CVA owing to an upstream trough in the growing season. The CVA regimes were more effective at bringing about

precipitation than the upsloping winter cases.

Overall, the meteorological analysis of the ten dry cases showed that the synoptic-scale flow regimes which bring about drought in the Canadian Prairies are more complex than was originally proposed by Dey (1982). There was no one flow regime that was distinct to the 1999–2005 Canadian Prairie drought, which makes these conditions even harder to predict. This drought did not disprove the traditional paradigm for Canadian Prairie drought – large-scale positive PNA ridging remains the most effective subsidence mechanism, particularly during the winter season. However, this analysis brought to light the great significance of downslope flow as a smaller-scale subsidence mechanism which, in the split-flow regime, was just as effective at bringing about subsidence and drought conditions as the traditional ridging paradigm. This analysis shows that drought conditions in the Canadian Prairies can be effectively maintained even without persistent strong amplitude positive PNA, since the downslope flow cases were characterized by weak PNA signal. In addition, this analysis showed that lack of moisture transport conducive to effective Prairie precipitation events (i.e. from the Gulf of Mexico) is not a first order cause of drought – there were dry cases with ample moisture transport from the Gulf of Mexico whose lifting was suppressed by the general synoptic-scale subsidence conditions. Low level moisture, however, is required for effective Prairie precipitation; all of the dry cases lacked this feature.

The synoptic study of the 1999–2005 drought reveals the extreme sensitivity of the Canadian Prairies to drought – it does not require one persistent pattern in order for meteorological drought to occur. This leads to the idea that this drought peaked in meteorological severity in 2001 and 2002 but was not a particularly exceptional meteorological drought when compared to the entire 1948–2005 period, an idea echoed in other studies (e.g. Bonsal and Regier 2007). Overall, however, it seemed that the great economic impacts of this drought did not match up to the degree of meteorological significance, pointing at a disconnect between the impact and the meteorology concerned. This idea of the impacts not agreeing with the severity of the natural event implies the larger issue that society is perhaps

increasing its vulnerability to natural hazards such as drought. It is very likely that the impact of the 1999–2005 Canadian Prairie drought was magnified by increased stress on the agricultural land, unsustainable farming practices, and too much reliance on precipitation as a source of crop moisture (as opposed to irrigation). With the changing climate and the expected poleward expansion of arid areas (Cook et al. 2010), it is inevitable that drought will still occur often in the Canadian Prairies. Whether these future droughts will be meteorologically unprecedented or not, perhaps the Canadian Prairie society should direct its efforts towards drought mitigation and adaptation in order to decrease its drought vulnerability, bringing the impacts closer in line with the meteorological significance.

Nevertheless, this study certainly motivates more research in the area of Canadian Prairie drought, particularly in a synoptic sense. The methods used in this study to combine the long-time scale condition (drought) with the shorter synoptic timescale were not without fault, but the resulting ability to diagnose subsidence mechanisms, and to further group the cases in terms of different dry regimes provides justification of this method. This methodology could be used to diagnose historical Canadian Prairie drought from 1948–present to continue the historical perspective and comparison with the 1999–2005 drought. In addition, high-low couplets of precipitation during Canadian Prairie drought, such as in the growing season of 2002, is worth additional study.

References

Agriculture and Agri-Food Canada, cited 2010: Drought watch prairie precipitation maps growing season 2002. [Available online at http://www.agr.gc.ca/pfra/drought/maps/archives/e2020830.pdf].

Alder, R. F., et al., 2003: The Version-2 Global Precipitation Climatology Project (GPCP) Monthly Precipitation Analysis (1979–Present). *J. Hydrometeor.*, **4**, 1147–1167.

Amante, C. and B. W. Eakins, 2009: ETOPO1 1 Arc-Minute Global Relief Model: Procedures, data sources and analysis. NOAA Technical Memorandum NESDIS NGDC-24, 19 pp.

American Meteorological Society, 2004: Meteorological Drought – Policy Statement. *Bull. Amer. Meteor. Soc.*, **85**.

American Meteorological Society, cited 2010: AMS Glossary of Meteorology, Second Edition. [Available online at http://www.cwb.ca/public/en/about/investor/annual/pdf/anneng.pdf].

Bluestein, H. B., 1992: *Synoptic-Dynamic Meteorology in Midlatitudes, Volume I: Principles of Kinematics and Dynamics*. Oxford University Press, Inc., 431 pp.

Bluestein, H. B., 1993: *Synoptic-Dynamic Meteorology in Midlatitudes, Volume II: Observations and Theory of Weather Systems*. Oxford University Press, Inc., 594 pp.

Bonsal, B. R., 2008: Droughts in Canada: An overview. *CMOS Bull.*, **36 (3)**, 79–86.

Bonsal, B. R. and A. K. Chakravarti, 1993: Teleconnections between North Pacific SST anomalies and growing season extended dry spells on the Canadian Prairies. *Int. J. Climatol.*, **13**, 865–878.

Bonsal, B. R. and R. G. Lawford, 1999: Teleconnections between El Niño and La Niña events and summer extended dry spells on the Canadian Prairies. *Int. J. Climatol.*, **19**, 1445–1458.

Bonsal, B. R. and M. Regier, 2007: Historical comparison of the 2001/2002 drought in the Canadian Prairies. *Clim. Res.*, **33**, 229–242.

Bonsal, B. R. and E. E. Wheaton, 2005: Atmospheric circulation comparisons between the 2001 and 2002 and the 1961 and 1988 Canadian Prairie Droughts. *Atmos.-Ocean*, **43 (2)**, 163–172.

Bonsal, B. R., X. Zhang, and W. D. Hogg, 1999: Canadian Prairie growing season precipitation variability and associated atmospheric circulation. *Clim. Res.*, **11**, 191–208.

Canadian Wheat Board, cited 2010a: Canadian Wheat Board 1995–96 Annual Report. [Available online at http://www.cwb.ca/public/en/about/investor/annual/pdf/anneng.pdf].

Canadian Wheat Board, cited 2010b: Canadian Wheat Board 2000–01 Annual Report Statistical Tables. [Available online at http://www.cwb.ca/public/en/about/investor/annual/pdf/2000-01_StatTables.pdf].

Canadian Wheat Board, cited 2010c: Canadian Wheat Board 2007–08 Annual Report Statistical Tables. [Available online at http://www.cwb.ca/public/en/about/investor/annual/pdf/07-08/stats_english2007-08.pdf].

Chipanshi, A. C., K. M. Findlater, T. Hadwen, and E. G. O'Brien, 2006: Analysis of consecutive droughts on the Canadian Prairies. *Clim. Res.*, **30**, 175–187.

Cook, E. R., R. Seager, R. R. Heim, R. S. Vose, E. Herweijer, and C. Woodhouse, 2010: Megadroughts in North America: Placing IPCC projections of hydroclimatic change in a long-term palaeoclimate context. *J. Quart. Sci.*, **25**, 48–61.

Dai, A., K. E. Trenberth, and T. Qian, 2004: A global dataset of Palmer Drought Severity Index for 1870–2002: Relationship with soil moisture and effects of surface warming. *J. Hydrometeor.*, **5**, 1117–1130.

Dale-Burnett, L., cited 2010: Palliser Triangle. [Available online at http://esask.uregina.ca/entry/palliser_triangle.html].

Dey, B., 1982: Nature and possible causes of droughts on the Canadian Prairies – case studies. *J. Climatology*, **2**, 233–249.

Doty, B., 1988: The Grid Analysis and Display System (GrADS), Version 2.0.a6. Center for Ocean-Land-Atmosphere Studies (COLA), Institute of Global Environment and Society (IGES).

Eady, E. T., 1949: Long waves and cyclone waves. *Tellus*, **1**, 33–52.

Evans, E. C., 2008: Canadian Prairie Drought: Characteristics of precipitation at the surfact and aloft with attendant atmospheric conditions for the summer months of 2001 and 2002. M.S. thesis, Department of Atmospheric and Oceanic Sciences, McGill University, 120 pp., [Available online at http://digitool.library.mcgill.ca/R/?func=dbin-jump-full&object_id=19267].

Groisman, P. Y. and D. R. Legates, 1994: The accuracy of United States precipitation data. *Bull. Amer. Meteor. Soc.*, **75 (3)**, 215–227.

Hayes, M., cited 2010: Drought indices. [Available online at http://drought.unl.edu/whatis/indices.htm].

Heim, R. R., 2002: A review of Twentieth-Century drought indices used in the United States. *Bull. Amer. Meteor. Soc.*, **83**, 1149–1165.

Hoerling, M. and A. Kumar, 2003: The perfect ocean for drought. *Science*, **299**, 691–694.

Hovmöller, E., 1949: The trough-and-ridge diagram. *Tellus*, **1**, 62–66.

Kalnay, E., et al., 1996: The NCEP/NCAR 40–year Reanalysis project. *Bull. Amer. Meteor. Soc.*, **77 (3)**, 437–471.

Karnauskas, K. B., A. Ruiz-Barradas, S. Nigam, and A. J. Busalacchi, 2008: North American Droughts in ERA–40 Global and NCEP North American Regional Reanalysis: A Palmer Drought Severity Index perspective. *J. Climate*, **21**, 2102–2123.

Kerr, R. A., 2000: A North Atlantic Climate Pacemaker for the Centuries. *Science*, **288 (5473)**, 1984–1986.

Knox, J. L. and R. G. Lawford, 1990: The relationship between Canadian Prairie dry and wet months and circulation anomalies in the mid-troposphere. *Atmos.-Ocean*, **28 (2)**, 189–215.

Liu, J., R. E. Stewart, and K. K. Szeto, 2004: Moisture transport and other hydrometeorological features associated with the severe 2000–2001 drought over the Western and Central Canadian Prairies. *J. Climate*, **17**, 305–319.

Mantua, N. J., S. R. Hare, Y. Zhang, J. M. Wallace, and R. C. Francis, 1997: A Pacific Interdecadal Climate Oscillation with impacts on salmon production. *Bull. Amer. Meteor. Soc.*, **78 (6)**, 1069–1079.

Maybank, J., B. Bonsal, K. Jones, R. Lawford, E. G. O'Brien, E. A. Ripley, and E. Wheaton, 1995: Drought as a natural disaster. *Atmos.-Ocean*, **33 (2)**, 195–222.

McCabe, G. J., M. A. Palecki, and J. L. Betancourt, 2004: Pacific and Atlantic Ocean influences on multidecadal drought frequency in the United States. *Proc. Natl. Acad. Sci. (USA)*, **101 (12)**, 4136–4141.

McKee, T. B., N. J. Doesken, and J. Kleist, 1993: The relationship of drought frequency and duration to time scales. *Eighth Conference on Applied Climatology*, Amer. Meteor. Soc., Anaheim, CA, 179–184.

Meehl, G. A., et al., 2007: Global climate projections. *Climate Change 2007: The Physical Science Basis. Contribution of Working Group I to the Fourth Assessment Report of the Intergovernmental Panel on Climate Change*, S. Solomon, D. Qin, M. Manning, Z. Chen, M. Marquis, K. B. Averyt, M. Tignor, and H. L. Miller, Eds., Cambridge University Press, Cambridge, United Kingdom and New York, NY, USA, 748–845.

Mekis, E. and W. D. Hogg, 1999: Rehabilitation and analysis of Canadian daily precipitation time series. *Atmos.-Ocean*, **37 (1)**, 53–85.

Mesinger, F., et al., 2006: North American Regional Reanalysis. *Bull. Amer. Meteor. Soc.*, **87**, 343–360.

Milrad, S. M., E. H. Atallah, and J. R. Gyakum, 2009: Dynamical and precipitation structures of poleward-moving tropical cyclones in Eastern Canada, 1979–2005. *Mon. Wea. Rev.*, **137**, 836–851.

Nkemdirim, L. and L. Weber, 1999: Comparison between the droughts of the 1930s and the 1980s in the Southern Prairies of Canada. *J. Climate*, **12**, 2434–2450.

Palmer, W. C., 1965: Meteorological drought. U.S. Weather Bureau Research Paper 45. 58pp, [Available from NOAA Library and Information Services Division, Washington, DC 20852].

Peixoto, J. P. and A. H. Oort, 1992: *Physics of Climate*. Springer-Verlag New York, Inc., 520 pp.

Phillips, D. W., 1990: *The Climates of Canada*. Environment Canada, 176 pp.

Quiring, S. M. and T. N. Papkryiakou, 2003: An evaluation of agricultural drought indices for the Canadian Prairies. *Agric. For. Meteor.*, **118**, 49–62.

Raddatz, R. L. and J. M. Hanesiak, 2008: Significant summer rainfall in the Canadian Prairie Provinces: modes and mechanisms 2000–2004. *Int. J. Climatol.*, **28**, 1607–1613.

Roberge, A., J. R. Gyakum, and E. H. Atallah, 2009: Analysis of intense poleward water vapor transports into high latitudes of Western North America. *Wea. Forecasting*, **24**, 1732–1747.

Ross, T. and N. Lott, 2003: A climatology of 1980–2003 extreme weather and climate events. NCDC Tech. Rep. 2003-01, US Department of Commerce, NOAA/NESDIS, NCDC, Asheville, NC 28801.

Seager, R., 2007: The turn of the century North American drought: Global context, dynamics, and past analogs. *J. Climate*, **20**, 5527–5552.

Shabbar, A., B. Bonsal, and M. Khandekar, 1997: Canadian precipitation patterns associated with the Southern Oscillation. *J. Climate*, **10**, 3016–327.

Shabbar, A. and W. Skinner, 2004: Summer drought patterns in Canada and the relationship to Global Sea Surface Temperatures. *J. Climate*, **17**, 2866–2880.

Shukla, J., et al., 2000: Dynamical Seasonal Prediction. *Bull. Amer. Meteor. Soc.*, **81 (11)**, 2593–2606.

St. George, S., et al., 2009: The Tree-Ring record of drought on the Canadian Prairies. *J. Climate*, **22**, 689–710.

Steinemann, A. C., M. J. Hayes, and L. F. N. Cavalcanti, 2005: Drought indicators and triggers. *Drought and Water Crises – Science, Technology, and Management Issues*, D. A. Wilhite, Ed., Taylor & Francis Group, Boca Raton, FL, 71–92.

Tannehill, I. R., 1947: *Drought: Its Causes and Effects*. Princeton University Press, Princeton, NJ, 597 pp.

Trenberth, K. E., et al., 2007: Observations: Surface and atmospheric climate change. *Climate Change 2007: The Physical Science Basis. Contribution of Working Group I to the Fourth Assessment Report of the Intergovernmental Panel on Climate Change*, S. Solomon, D. Qin, M. Manning, Z. Chen, M. Marquis, K. B. Averyt, M. Tignor, and H. L. Miller, Eds., Cambridge University Press, Cambridge, United Kingdom and New York, NY, USA, 237–336.

Wallace, J. M. and D. S. Gutzler, 1981: Teleconnections in the Geopotential Height Field during the Northern Hemisphere Winter. *Mon. Wea. Rev.*, **109**, 784–812.

Weber, L. and L. Nkemdirim, 1998: Palmer's drought indices revisited. *Geografiska Ann.*, **80 A (2)**, 153–172.

Wheaton, E., S. Kulshreshtha, V. Wittrock, and G. Koshida, 2008: Dry times: hard lessons from the Canadian drought of 2001 and 2002. *Can. Geog.*, **52 (2)**, 241–262.

Wilhite, D. A. and M. Buchanan-Smith, 2005: Drought as hazard: Understanding the natural and social context. *Drought and Water Crises – Science, Technology, and Management Issues*, D. A. Wilhite, Ed., Taylor & Francis Group, Boca Raton, FL, 1–29.

World Meteorological Organization, cited 2010: Lincoln declaration on drought indices. [Available online at http://snr.unl.edu/download/aboutus/what/newsarchive/WMOConference2009NebraskaDeclarationonDroughtIndicesFinal.pdf].